Light-Driven Anaerobic Microbial Oxidation of Manganese

Mirna Daye[1], Vanja Klepac-Ceraj[2], Mihkel Pajusalu[1], Sophie Rowland[2], Anna Farrell-Sherman[2], Nicolas Beukes[3], Nobumichi Tamura[4], Gregory Fournier[1], Tanja Bosak[1]

Affiliations:

[1]Department of Earth, Atmospheric, and Planetary Sciences, Massachusetts Institute of Technology, Cambridge, Massachusetts 02139.

[2]Department of Biological Sciences, Wellesley College, 106 Central St, Wellesley, Massachusetts 02481.

[3] DST-NRF CIMERA, Geology Department, University of Johannesburg, Auckland Park, 2006, South Africa.

[4]Advanced Light Source, Lawrence Berkeley National Laboratory, Berkeley, California 94720,

Oxygenic photosynthesis supplies organic carbon to the modern biosphere, but it is uncertain when this metabolism originated. Based on the inferred presence of manganese oxides in the sediments as old as 3 billion years, it has been proposed that photosynthetic reaction centers capable of splitting water arose by that time. However, this assumes that manganese oxides can only be produced in the presence of molecular oxygen[1], reactive oxygen species[2,3] or by high-potential photosynthetic reaction centers[4,5]. Here we show that anoxygenic photosynthetic microbial communities biomineralize manganese oxides under strictly anaerobic conditions and in the absence of high-potential photosynthetic reaction centers. Microbial oxidation of Mn(II) in the absence of molecular oxygen during the Archean Eon would have produced geochemical signals identical to those used to date the evolution of oxygenic photosynthesis before the Great Oxidation Event (GOE)[6,7]. This light-dependent process may also produce manganese oxides in the photic zones of modern anoxic water bodies and sediments.

Manganese (Mn) and more than 30 of its described oxides and hydroxides mediate the cycling of various trace metals and nutrients in the environment. The ability of microbes to oxidize Mn(II) anaerobically is also hypothesized to have been a critical step in the evolution of oxygenic photosynthesis on the early Earth[4]. However, modern microbes are not known to anaerobically oxidize manganese. Here, we demonstrate this activity in active microbial cultures that grow in the presence of nanomolar oxygen concentrations relevant for the Archean Earth.

Inoculum for the enrichment cultures of strictly anaerobic, photosynthetic biofilms came from the meromictic Fayetteville Green Lake (FGL), NY. The anaerobic photic zone of the lake contains 20 nM to 61 μM Mn(II) and 0-0.04 mM of H_2S [8], and the most abundant phototroph there is the green sulfur bacterium *Chlorobium* sp.[9]. This microbe uses sulfide, hypothesized to be the oldest electron donor for photosynthesis[10], as an electron donor. Photosynthetic biofilms of this organism and other strict anaerobes (Fig. 1a) were enriched in a minimal medium amended with 20-50 μM Na_2S and 1 mM $MnCl_2$ and equilibrated with an anaerobic atmosphere of 80% N_2 and 20% CO_2 at pH 7. The concentration of O_2 in the medium was lower than 2 nM during the entire experiment, both in the presence and the absence of cells (see Methods and Extended Data Fig. 1). These experimental concentrations match the upper estimates for the Archean Earth[11]. The anaerobic medium also lacked other potential oxidants for Mn(II) such as nitrite, nitrate and H_2O_2 and these species were not produced in sterile controls (Extended Data Section 5).

Four times more biomass grew in photosynthesizing cultures relative to the cultures incubated in the dark (*p*-value << 0.001; Fig. 1b). The enrichment protocol removed all typical biological sources of oxygen such as cyanobacteria and photosynthetic eukaryotes from the original inoculum and all of the subsequent transfers (Fig. 1c). The resulting community was stable and contained *Chlorobium*, *Paludibacter*, *Acholeplasma*, *Geobacter*, *Desulfomicrobium*, *Clostridium*, *Acetobacterium*, and several other bacteria. The *Chlorobium* sp. was the most abundant taxon across all conditions, as well as the only identifiable phototroph (Fig. 1c). Its genome was 98.4% similar to *Chlorobium limicola* Frassasi.

These microbial communities were essential to the precipitation of minerals and oxidation of manganese. Mn-rich dolomite was the most abundant precipitate in photosynthetic cultures amended with 0.1-1 mM Mn(II) and 20-250 μM sulfide (Fig. 2, Extended Data Fig. 5a, b, d)[14], which is in the 0.1 mM range of dissolved Mn(II) concentrations thought to have been maintained by precipitation of Mn-containing carbonate minerals on the Archean carbonate platforms[12,13]. Cultures incubated in this range of chemical conditions also contained manganese oxide minerals (Figs. 1d, 2), but those incubated with ~1 μM Mn(II) or 1 mM sulfide did not (Extended Data Fig. 5c). Precipitates were entirely absent from sterile controls incubated in the light, whereas minor calcite, less dolomite and no manganese oxides were detected in cultures shielded from the light (Fig. 2). Elemental S^0 accumulated in cultures that did not contain oxidized manganese minerals (Extended Data Figs. 5c and 6), as expected when *Chlorobium* sp. grows on sulfide as the main photosynthetic electron donor (Extended Data Fig. 7). The lack of oxidized manganese in sterile controls showed that abiotic oxidation reactions did not contribute detectable amounts of manganese oxides under our experimental conditions. Thus, the microbial presence and photosynthetic activity strongly controlled the nucleation and precipitation of minerals, including manganese oxides, under our experimental conditions.

To characterize the redox cycling of manganese, we examined its oxidation state by surface-sensitive methods (Extended Data Figs. 2, 3). After two weeks, sterile controls and cultures that were incubated in the dark contained only Mn(II) (Extended Data Figs. 2 and 3a). Dolomite that formed in photosynthetic cultures contained Mn(II)[14], but Mn(II), Mn(III) and Mn(IV) in calcium manganese oxides, Mn_3O_4 and other minerals were also detected (Figs. 1d, 2; Fig. 3, Extended Data Figs. 3, 4). The presence of manganese oxides in sulfidic photosynthetic cultures was surprising (Fig. 2), but we detected them repeatedly in biofilms that were two weeks to two months old (Fig. 2). A colorimetric assay quantified 5.1 ± 0.8 μM of oxidized manganese in one-week-old biofilms, 7.2 ± 0.8 μM oxidizing equivalents in two-week-old biofilms to > 10 μM in three-week old biofilms (Methods 6). All oxidized manganese was determined as $KMnO_4$ equivalents and none was detected in dark controls.

Oxidized manganese was present in minerals that formed directly at the surfaces of cells (Fig. 3a). These cells could be identified as *Chlorobium* sp. based on the presence of large intracellular complexes of photosynthetic antennae called chlorosomes (Fig. 3b) and surface protrusions called spinae[15]. Notably, minerals were only found on cell surfaces and never around chlorosomes, pointing to the involvement of cell surfaces and periplasmic processes in manganese oxidation. High-resolution transmission electron micrograph of fresh cell suspensions showed Mn-Ca minerals with a uniform lattice fringe that corresponded to (121) plane with interplanar spacing of 2.64 Å of calcium manganese oxide (Fig. 3d), Mn_3O_4 (Fig. 3f) and other manganese minerals (Extended Data Fig. 3, 4). Extracellular vesicles, spinae and manganese

oxide minerals were absent from *Chlorobium* sp. when the cultures were incubated with Mn(II) in the dark or photosynthetically with 1 mM sulfide.

Light-driven manganese oxidation occurred only when *Chlorobium* sp. and other microbes, including *Geobacter* sp., were growing together. Oxidized manganese was present in enrichment cultures of microbes from FGL that contained *Chlorobium* sp, *Geobacter sp., Acholeplasma equifetale, Alistipes sp. HGB5, and Caldicoprobacter oshimai*, but absent from co-cultures of *Chlorobium* sp. and *Desulfomicrobium* sp. (Extended Data Fig. 8) and pure cultures of *Chlorobium limicola*. To identify the simplest co-cultures that could oxidize manganese, we tested for the presence of manganese oxidizing activity in co-cultures of isolated strains of *C. limicola, Chlorobaculum tepidum* and *Geobacter lovleyi* (DSM 245, DSM 12025 and DSM 17278, DSMZ GmbH Germany) (Extended Data 2.3.1). Manganese oxidizing activity was detected only in the co-cultures containing all three organisms and the co-cultures of *C. limicola* and *G. lovleyi* (Extended Data Fig. 9), suggesting that the activity may depend on extracellular electron transfer between the latter two organisms[16] by a currently unknown mechanism. The genome of *Chlorobium* sp. encodes only a well-studied photosynthetic reaction center with the midpoint potential around +250 mV[17] that cannot directly oxidize Mn(II)-bicarbonate (Eh = 520-670 mV)[4,18]. *Chlorobium* sp. also lacks clear homologs of proteins known to oxidize manganese under aerobic conditions[19-21]. Manganese oxidation in *C. limicola* may occur by an endergonic mechanism analogous to that proposed for the oxidation of nitrite by *Thiocapsa* sp. strain KS1[22], but Mn(II) oxidation process and potential oxidants in the co-cultures of *C. limicola* and *G. lovleyi* remain to be characterized. The electron transfer between *C. limicola* and *G. lovleyi* may involve high potential cytochrome c in *Chlorobium* sp. and OmpB operating in reverse in *Geobacter* sp.

The abundance of oxidized manganese in microbial biofilms and its absence from the sterile controls shows that microbial consortia can mediate the precipitation of manganese oxide minerals under Archean-like conditions. These findings expand the diversity of minerals and redox processes beyond what was thought possible in strictly anaerobic environments or in the presence of high-potential photosynthetic reaction centers. Microbial interactions that mediate the light-dependent redox cycling of manganese and couple it to other elemental cycles remain to be identified, but can be expected in modern environments where light, sulfide and dissolved Mn(II) coexist, but sulfide concentrations do not exceed ~ 0.2 mM (Extended Data Table 1). Light dependent microbial production of manganese oxides is likely to stimulate the redox cycles of carbon, sulfur, nitrogen and iron and increase the diversity of anaerobic redox transformations, including nitrification-denitrification[23], with implications for the interpretation of isotopic and chemical signatures of these processes in modern anaerobic settings.

The biological production of manganese oxides under Archean-like chemical conditions has additional major implications for determining the timing of the origin of oxygenic photosynthesis, which is currently debated[5-7]. The evolution of oxygenic photosynthesis[6] and the presence of locally oxic areas in the pre-GOE, Archean marine systems[24] are inferred from geochemical signals. However, interpretations of these signals assume the former presence of manganese oxides[6,7,25,26]. For example, manganese carbonate deposits with the negative $\delta^{13}C$ values reported in the Neoarchean Sandur Schist belt in India[27] or Mesoarchean Witwatersrand-Mozaan strata in South Africa[24,25] are thought to have been produced by the microbial reduction of Mn(III) and Mn(IV)-oxide minerals. In turn, these oxides are attributed to the aerobic

oxidation of Mn(II) in the presence of oxygen. Molecular clock models are used to independently time the evolution of the crown group cyanobacteria, with estimates that range from before 3 billion years ago (Ga) to after the GOE, depending on sequence datasets, prior assumptions and specific model calibrations[28]. These models support the radiation of anoxygenic green sulfur bacteria (GSB) such as *Chlorobium* and green non-sulfur bacteria (GSN) after the GOE[28], but also show that stem GSB diverged as early as 2.9 Ga. Given that the last common ancestor of modern GSB was photosynthetic, model estimates are consistent with anoxygenic photosynthesis within stem GSB long before the GOE (also see Extended data Fig. 11). Therefore, given that anaerobic manganese oxidation requires anoxygenic photosynthetic activity in the presence of sulfide, this process could be as old as anoxygenic phototrophic ancestors of any extant groups of phototrophs, such as GSB, Cyanobacteria, or even an extinct lineage of anoxygenic phototrophs. Because any of these scenarios can predate the GOE, the relative contributions of anaerobic and oxygen-dependent Mn(II) oxidation to the redox texture of sedimentary rocks much before the GOE[29] are an open question and the loss of mass-independent sulfur isotope signals at GOE[30] remains the firmest evidence for biological production of oxygen.

References

1 Tebo, B. M. *et al.* Biogenic manganese oxides: properties and mechanisms of formation. *Annu. Rev. Earth Planet. Sci.* **32**, 287-328 (2004).

2 Oze, C., Sleep, N. H., Coleman, R. G. & Fendorf, S. Anoxic oxidation of chromium. *Geology* **44**, 543-546 (2016).

3 Liang, M.-C., Hartman, H., Kopp, R. E., Kirschvink, J. L. & Yung, Y. L. Production of hydrogen peroxide in the atmosphere of a Snowball Earth and the origin of oxygenic photosynthesis. *Proc. Natl. Acad. Sci. U S A.* **103**, 18896-18899 (2006).

4 Dismukes, G. C. *et al.* The origin of atmospheric oxygen on Earth: the innovation of oxygenic photosynthesis. *Proc. Natl. Acad. Sci. U S A.* **98**, 2170-2175, doi:10.1073/pnas.061514798 (2001).

5 Johnson, J. E. *et al.* Manganese-oxidizing photosynthesis before the rise of cyanobacteria. *Proc. Natl. Acad. Sci. USA.* **110**, 11238-11243 (2013).

6 Planavsky, N. J. *et al.* Evidence for oxygenic photosynthesis half a billion years before the Great Oxidation Event. *Nature Geosci.* **7**, 283-286 (2014).

7 Crowe, S. A. *et al.* Atmospheric oxygenation three billion years ago. *Nature* **501**, 535-538 (2013).

8 Havig, J. R., McCormick, M. L., Hamilton, T. L. & Kump, L. R. The behavior of biologically important trace elements across the oxic/euxinic transition of meromictic Fayetteville Green Lake, New York, USA. *Geochim. Cosmochim. Acta.* **165**, 389-406 (2015).

9 Culver, D. A. & Brunskill, G. J. Fayetteville Green Lake, New York. V. Studies of primary production and zooplankton in a meromictic marl lake. *Limnol. Oceanogr.* **14**, 862-873, doi:10.4319/lo.1969.14.6.0862 (1969).

10 Martin, W. F., Bryant, D. A. & Beatty, T. J. A physiological perspective on the origin and evolution of photosynthesis. *FEMS Microbiol. Rev.* **42**, 205-231 (2018).

11 Pavlov, A. A. & Kasting, J. F. Mass-independent fractionation of sulfur isotopes in Archean sediments: Strong evidence for an anoxic Archean atmosphere. *Astrobiology* **2**, 27-41, doi:Doi 10.1089/153110702753621321 (2002).
12 Anbar, A. D. & Holland, H. D. The photochemistry of manganese and the origin of banded iron formations. *Geochim. Cosmochim. Acta* **56**, 2595-2603 (1992).
13 Beukes, N. J. Facies relations, depositional environments and diagenesis in a major early proterozoic stromatolitic carbonate platform to basinal sequence, Campbellrand Subgroup, Transvaal Supergroup, Southern Africa. *Sediment Geol* **54**, 1-46 (1987).
14 Daye, M., Higgins, J., Bosak, T. Formation of ordered dolomite in anaerobic photosynthetic biofilms. *Geology*. doi: https://doi.org/10.1130/G45821.1 (2019).
15 Pibernat, I. & Abella, C. Sulfide pulsing as the controlling factor of spinae production in *Chlorobium limicola* strain UdG 6038. *Arch. Microbiol.* **165**, 272-278 (1996).
16 Ha, P. T. *et al.* Syntrophic anaerobic photosynthesis via direct interspecies electron transfer. *Nat Commun.* **8**, 1-7 (2017).
17 Prince, R. C. & Olson, J. M. Some thermodynamic and kinetic properties of the primary photochemical reactants in a complex from a green photosynthetic bacterium. *Biochim. Biophys. Acta-Bioenergetics* **423**, 357-362 (1976).
18 Dasgupta, J., Tyryshkin, A. M., Kozlov, Y. N., Klimov, V. V. & Dismukes, G. C. Carbonate complexation of Mn^{2+} in the aqueous phase: redox behavior and ligand binding modes by electrochemistry and EPR spectroscopy. *J. Phys. Chem. B.* **110**, 5099-5111 (2006).
19 Butterfield, C. N., Soldatova, A. V., Lee, S.-W., Spiro, T. G. & Tebo, B. M. Mn (II, III) oxidation and MnO_2 mineralization by an expressed bacterial multicopper oxidase. *Proc. Natl. Acad. Sci. USA.* **110**, 11731-11735 (2013).
20 Geszvain, K., Smesrud, L. & Tebo, B. M. Identification of a third Mn (II) oxidase enzyme in *Pseudomonas putida* GB-1. *Appl. Environ. Microbiol.* **82**, 3774-3782 (2016).
21 Andeer, P. F., Learman, D. R., McIlvin, M., Dunn, J. A. & Hansel, C. M. Extracellular haem peroxidases mediate Mn (II) oxidation in a marine *Roseobacter* bacterium via superoxide production. *Environ. Microbiol.* **17**, 3925-3936 (2015).
22 Hemp, J. *et al.* Genomics of a phototrophic nitrite oxidizer: insights into the evolution of photosynthesis and nitrification. *ISME J.* **10**, 2669–2678 (2016).
23 Hulth, S., Aller, R. C. & Gilbert, F. Coupled anoxic nitrification/manganese reduction in marine sediments. *Geochimica et Cosmochimica Acta* **63**, 49-66 (1999).
24 Kurzweil, F., Wille, M., Gantert, N., Beukes, N. J. & Schoenberg., R. Manganese oxide shuttling in pre-GOE oceans – evidence from molybdenum and iron isotopes. *Earth Planet. Sci. Lett.* **452**, 69-78 (2016).
25 Ossa, F. O., Hofmann, A., Vidal, O., Kramers, J. D. & Cavalazzi, G. Unusual manganese enrichment in the Mesoarchean Mozaan Group, Pongola Supergroup, South Africa. *Precambrian. Res.* **281**, 414-433 (2016).
26 Beukes, N. J., Gutzmer, J. & Nel, B. Ce anomalies in similar to 2.4 Ga iron and manganese formations as proxy for early oxygenation of oceanic environments. *Geochim. Cosmochim. Acta.* **74**, A85-A85 (2010).

27 Manikyamba, C. & Naqvi, S. M. Geochemistry of Fe-Mn formations of the Archaean Sandur schist belt, India - mixing of clastic and chemical processes at a shallow shelf. *Precamb. Res.* **72**, 69-95 (1995).
28 Magnabosco, C., Moore, K. R., Wolfe, J. M. & Fournier, G. P. Dating phototropic microbial lineages with reticulate gene histories. *Geobiology* **16**, 179-189 (2018).
29 Hazen, R. M. *et al.* Mineral evolution. *Am. Mineral.* **93**, 1693- 1720 (2008).
30 Bekker, A. *et al.* Dating the rise of atmospheric oxygen. *Nature* **427**, 117–120 (2004).

Supplementary Information is available in the online version of the paper.

Acknowledgments: We thank the current members of the Bosak laboratory and acknowledge the support by Simons Foundation Collaboration on the Origins of Life (327126 to TB) and FESD NSF project #1338810 (TB). Part of this work was performed in MIT Center for Material Science and Engineering; part of Materials Research Science and Engineering Center funded by National Science Foundation under award number DMR-1419807. Some analyses were carried out at the Harvard University Center for Nanoscale Systems (CNS), a member of the National Nanotechnology Coordinated Infrastructure Network (NNCI) supported by the National Science Foundation under NSF ECCS award no. 1541959. This research used BI L12.3.2, a resource of the Advanced Light Source, which is a DOE Office of Science User Facility under contract no. DE-AC02-05CH11231. MP received funding from John Templeton foundation and the Professor Amar G. Bose Research Grant Program, MIT.

Author Contributions M.D. and T.B. conceived and designed the project, conducted pilot studies and collected preliminary data. M.D., S.R., N.T and M.P. performed the experiments. V.K.-C, A.F.-R. and S.R. analyzed microbial communities and performed bioinformatic analyses. M.D and T.B wrote the manuscript with input from M.P. and V.K.-C., and N.B. All co-authors reviewed and approved the final manuscript.

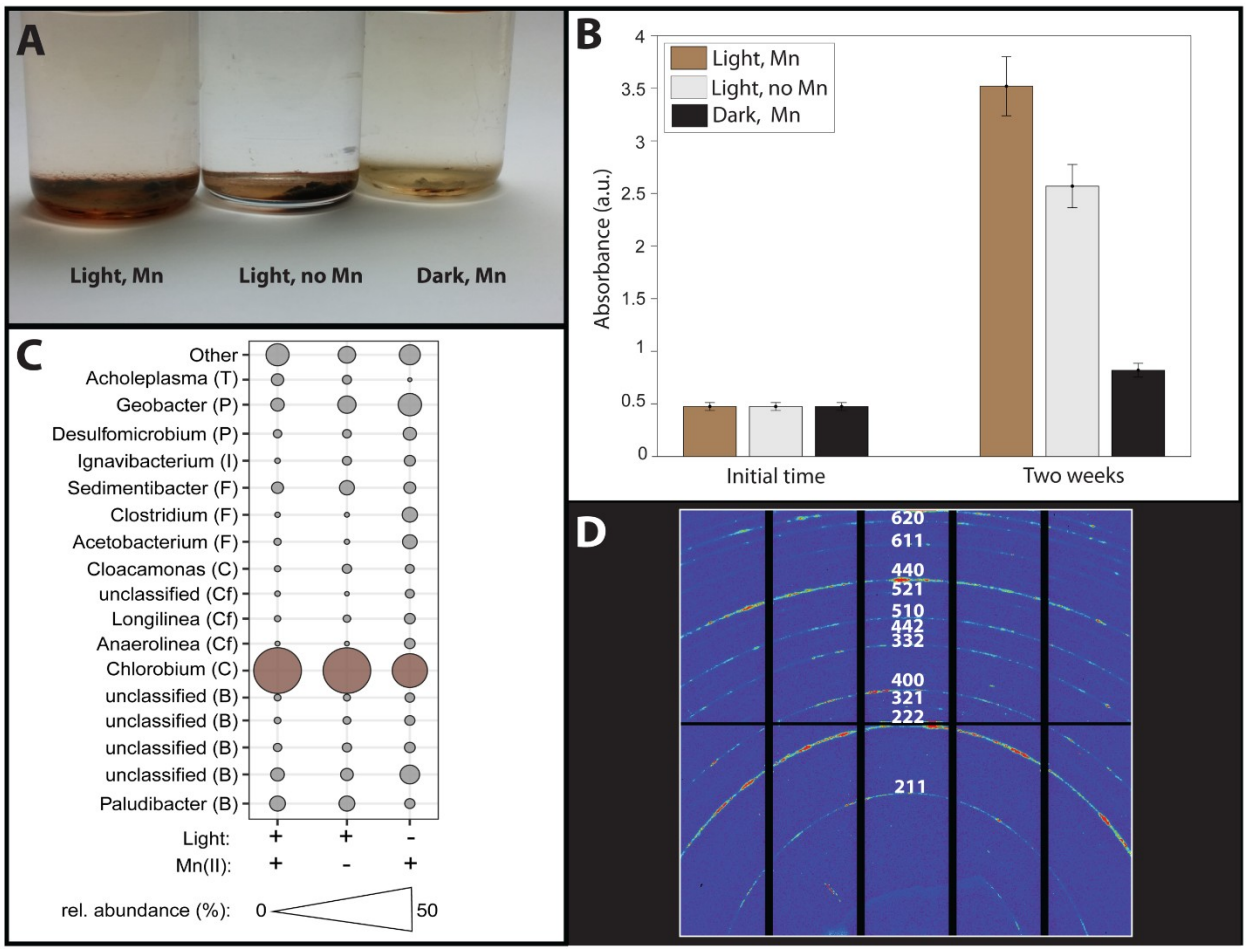

Figure 1. Biofilms incubated for two weeks. A: Dark brown biofilm incubated in the light with Mn(II) covers the entire bottom of the culture bottle. Biofilm incubated in the light without Mn(II) covers only a portion of the bottom. Biofilm incubated in the dark with Mn(II) is yellow. B: Biomass of biofilms measured by the crystal violet assay. All incubations were performed in triplicate. C: Microbial diversity in biofilms obtained by high-throughput Illumina sequencing of 16S rRNA genes. The most abundant taxon across all conditions was a *Chlorobium* sp. (30-60%). This microbe was more abundant in photosynthesizing cultures (Extended Data). D: Diffraction pattern indexes for Mn_3O_4 in the spectrum acquired by synchrotron micro-focused X-ray diffraction (μXRD) of a biofilm incubated in the light for two weeks.

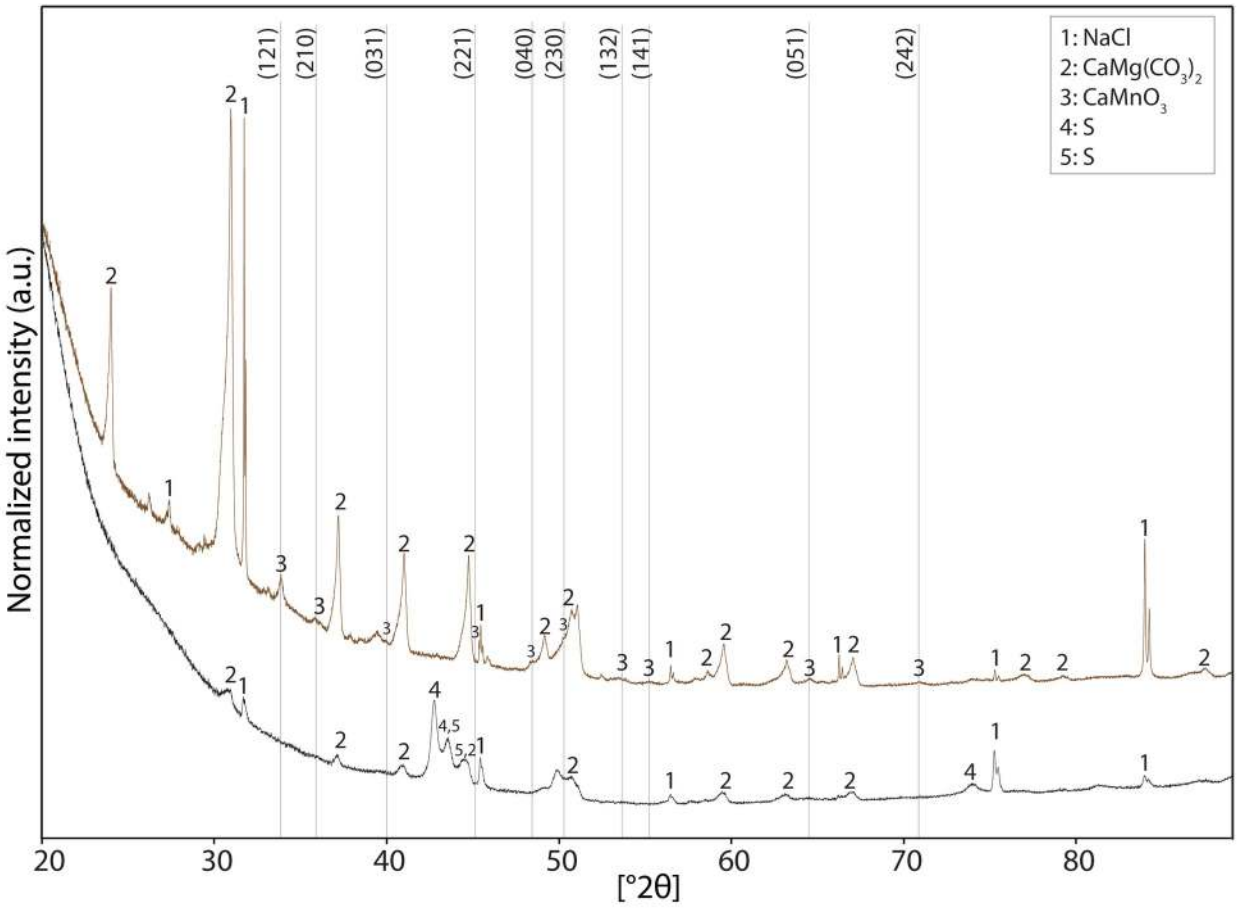

Figure 2. X-ray diffraction spectra (XRD) of biofilms incubated for two weeks. Top spectrum: biofilms incubated in the light with 1 mM Mn(II). Black lines indicate Miller indices (*hkl*) assigned to each peak of $CaMnO_3$. Bottom spectrum: biofilms incubated in the dark with 1 mM Mn(II). Biofilm incubated in the dark contains sulfur phases (S, "4" and "5") that formed during the treatment to remove oxidized manganese minerals before inoculation (see Methods 1.1.1., Extended Data Fig. 10 and Methods 3.2 for the interpretation of XRD peaks).

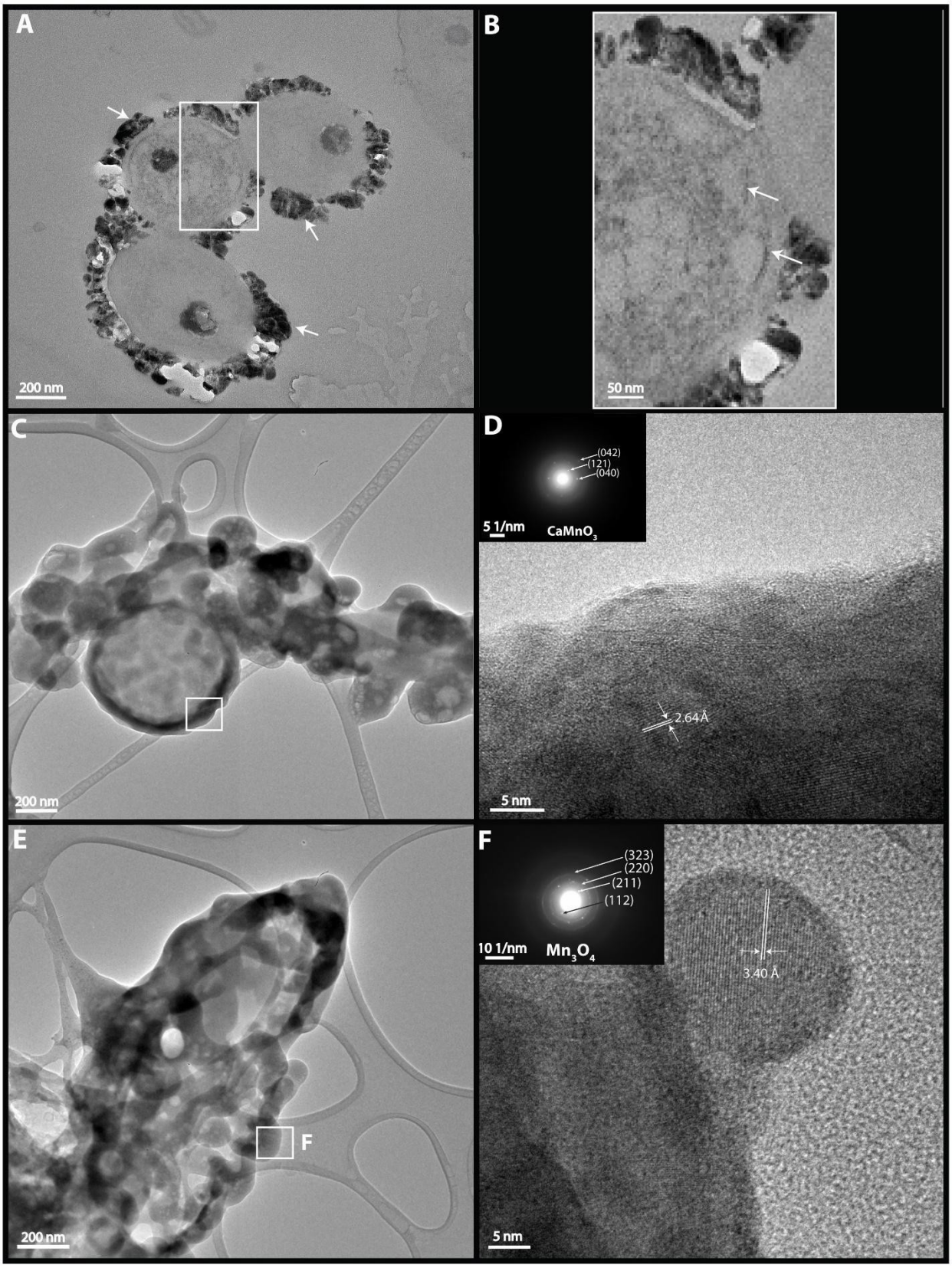
A
200 nm
B
50 nm
C
200 nm
D
(042)
(121)
(040)
5 1/nm
CaMnO3
2.64Å
5 nm
E
F
200 nm
F
(323)
(220)
(211)
(112)
10 1/nm
Mn3O4
3.40 Å
5 nm

Figure 3. Microbe-mineral interactions in biofilms incubated with Mn(II) in the light for two weeks. A: Mineral-encrusted cells (white arrows) in fixed and stained samples (TEM at 80 kV); white square indicates the area magnified in panel B. B: Chlorosomes (white arrows) in a cell that is encrusted by manganese oxide precipitates (TEM at 80 kV, fixed and stained sample). C: TEM at 200 kV of unprocessed and unstained microbial cells. Minerals encrust the cell envelope. White squares indicate the regions selected for SAED shown in panel D. D: High resolution TEM and selected area electron diffraction (SAED) of minerals around an unstained cell from a fresh suspension of the microbial culture on a TEM grid. The indexes of the SAED pattern correspond to $CaMnO_3$ with the d-spacing of 2.64 Å. E: TEM at 200 kV of unprocessed and unstained microbial cells. Minerals encrust the surface of the cell. White square indicates the region selected for SAED shown in panels F. F: HRTEM and SAED of minerals in the area outlined by the white square in E. The indexes of the SAED pattern correspond to Mn_3O_4 with d-spacing of 3.40 Å.

METHODS

1. Culturing and sequencing

1.1. Enrichment and culturing conditions

Sediments were retrieved from Fayetteville Green Lake (FGL) by a metallic gravity scoop and stored at 4°C in fully filled, hermetically sealed glass jars. These samples were used as inoculum for enrichment cultures in the FGL medium described below. All inoculations were conducted in an anaerobic chamber under a 5%CO_2: 5%H_2: balN_2 (v/v/v) atmosphere using standard anaerobic techniques[31]. Briefly, FGL medium was flushed before and after autoclaving in hermetically sealed glass bottles. Sterile flushed FGL medium was inoculated inside the anaerobic chamber (5% H_2/15% CO_2/80% N_2 atmosphere). To avoid any issues associated with the exposure of biofilms to H_2, the serum bottles were opened inside the anaerobic chamber, inoculated in about 1 minute, closed immediately, capped and flushed again with CO_2/N_2 for 60-75 minutes to remove H_2. All experiments were conducted in batch cultures and all cultures were inoculated by approximately 1 mg of biofilm that had been washed six times by anoxic nanopure water[32,33], mechanically dispersed by passing through a syringe and resuspended in sterile anaerobic medium. All these steps were carried out in the anaerobic glove box. All enrichment cultures were incubated at 27°C with incandescent white light bulb and a 12:12h day/night cycle. All enrichment cultures were incubated at 27°C with incandescent white light bulb and a 12:12h day/night cycle. All plasticware used in the anaerobic chamber was introduced into the chamber at least one week before the experiments.

The culture medium (FGL medium) contained: 0.1 mM KH_2PO_4, 5.61 mM NH_4Cl, 0.9 mM KCl, 0.024 M $NaHCO_3$, 1 mM $MnCl_2.2\ H_2O$, 1 mM Na_2SO_4, 1 ml/L of trace element solution. The trace element solution was prepared in 10% (v/v) HCl and contained per liter; 1.5 g $FeCl_2.4H_2O$, 190 mg $CoCl_2.6H_2O$, 100 mg $MnCl_2.4H_2O$, 70 mg $ZnCl_2$, 31 mg Na_2MoO_4, 6 mg H_3BO_3, 2 mg $CuCl_2.2H_2O$. The pH of the medium was adjusted to 7 by the addition of NaOH (1M) or HCl (1 M). After adjusting the pH to 7, the FGL medium was distributed into glass bottles of different volumes (12, 25, 50, 150, 200 mL). The final background concentration of manganese was 0.4 μM. To inhibit the growth of oxygenic phototrophs, we added 0.01 mM DCMU (3-(3,4-dichlorophenyl)-1,1-dimethylurea) to the initial enrichments. All analyses described in the main text used later enrichments that were grown in DCMU-less media. Glass serum bottles were capped by butyl rubber stoppers and aluminum seals. Before autoclaving, the FGL medium in bottles were flushed by 20% CO_2: 80% N_2 for one hour, the serum bottle headspaces for another 40 minutes total. The bottles were then autoclaved (40 minutes sterile). After autoclaving, the FGL medium in bottles were flushed again by 20% CO_2: 80% N_2 for one hour, the serum bottle headspaces for another 40 minutes total after cooling.

A separately prepared selenium stock solution contained 2 mg of Na_2SeO_3 in 1000 mL of 0.01 M NaOH. This solution was autoclaved and made anaerobic by flushing the bottles for 1 hr and 40 min with 20% CO_2: 80% N_2. The vitamin solution was prepared in nanopure water by aerobic filter sterilization and contained per liter: 2 mg biotin, 2 mg folic acid, 10 mg pyridoxine-$2H_2O$, 5 mg thiamine-HCl-$2H_2O$, 5 mg riboflavin, 5 mg nicotinic acid, 5 mg D-Ca-pantothenate, 0.1 mg vitamin B12, 5 mg p-aminobenzoic acid, 5 mg lipoic acid.

The master stock solution (20x) contained 1.5 mM $MgCl_2.6H_2O$, 1 mM $CaCl_2.2\ H_2O$, 1 mL of vitamin solution and 1 ml of the selenium stock solution in 50 mL nanopure water. The master solution was filter-sterilized and flushed for 1 hr and 40 min by 20% CO_2: 80% N_2 gas

mixture. This solution was added to the FGL medium immediately before inoculation, 5 mL per 100 ml medium. Manganese was added at the time of inoculation from concentrated anerobic stock solution of $MnCl_2.4H_2O$ (1 M). Finally, after inoculation, the medium was reduced by the addition of sulfide from a concentrated anaerobic stock solution of $Na_2S.5H_2O$ (0.2 M).

The medium used for the initial enrichment was reduced by the addition of 4 mM sodium ascorbate instead of sulfide to minimize the growth of organisms that require high concentrations of sulfide as an electron donor. A brown microbial mat formed on the surface of the inoculated sediments after 3-4 weeks. Fragments of this mat were transferred into the sterile medium with the same composition as described above, incubated in the same conditions for one month, and transferred again. All experiments described here used biofilms that had undergone at least four transfers from the initial enrichment.

1.1.1. Modified FGL medium. All experiments described in the main text used the modified basal FGL (MFGL) medium. This medium did not contain DCMU, sulfate or ascorbate, and was reduced by 20-50 μM Na_2S. Sterile MFGL contained only traces of sulfate (< 0.9 μM), nitrate (< 0.5 μM) and nitrite (< 0.1 μM), as detected by ion chromatography (see section 5).

To evaluate the influence of light on growth, biofilms from the third transfer were inoculated into the MFGL medium. One triplicate set of batch cultures was incubated for two weeks in the light at 27°C at a distance of 35 cm from an incandescent white light bulb that emits between 400-700 nm. Another set was incubated at the same time and at the same temperature but was shielded from the light by aluminum foil.

To reduce the carryover of manganese oxides in the biofilm inoculum, we reduced the inoculums using a previously described protocol[34]. Briefly, microbial biofilms that had been grown in the presence of light and 1 mM Mn(II) were harvested and incubated in anaerobic sterile ascorbic acid (0.25 mM) in the anaerobic chamber for 10 minutes. After this incubation, the biofilms were washed three times with sterile, anaerobic nanopure water. XRD analyses of biofilms treated in this manner showed that this protocol removed manganese oxide minerals but increased the abundance of elemental sulfur in the inoculum (Extended Data Fig. 10). Elemental sulfur was absent from the biofilms before the treatment (Fig. 2a).

To characterize the effect of different initial concentrations of manganese and sulfide on mineral precipitation, biofilms from the third transfer of the original enrichment culture were inoculated into the MFGL medium amended by $MnCl_2$, and Na_2S from 0.5 M and 0.1 M anaerobic stock solutions. All stock solutions were prepared, autoclaved and stored under an atmosphere of N_2. The effect of Mn concentration on manganese oxidation was evaluated in three sets of triplicate inoculated cultures that contained 0.1, 1 or 5 mM $MnCl_2$. All these cultures were reduced with 50 μM Na_2S. The effect of H_2S concentration on manganese oxidation was explored in three sets of triplicate cultures reduced by 0.05, 0.25 or 1 mM of Na_2S, all amended with 1 mM $MnCl_2$. An additional set of triplicate cultures contained 1 mM Mn(II) and 0.02 mM Na_2S. All cultures were incubated for two weeks.

1.2. Further enrichment of Mn-oxidizing and sulfide-oxidizing microbes

Microbial communities capable of anaerobic oxidation of manganese were further enriched by inoculating anaerobically sealed agar shake tubes with the dispersed biofilms, serially diluting the cultures in agar, transferring colonies into liquid medium and repeating the entire process for

the second time[35,36]. The MFGL medium in agar shake tubes was solidified by 1.1 % agar. Biofilms were washed with anaerobic nanopure water in the anaerobic glove box and mechanically dispersed in 10 ml of the basal MFGL medium. The first agar shake tube was inoculated with 10% (1 ml) of the dispersed inoculum and diluted by five successive transfers of 1 ml into 9 ml of sterile MFGL.

The additions of sulfide and manganese to the basal MFGL in agar shake tubes targeted two different conditions: Condition 1) 0.02 mM Na_2S and 1 mM $MnCl_2$ sought to enrich for microbes that can photosynthesize in the presence of low sulfide concentrations and oxidize Mn(II); Condition 2) 1 mM Na_2S ($MnCl_2$ added only in the trace metal solution) enriched for *Chlorobium spp*. that can oxidize sulfide. Extended Data Table 2 summarizes the enrichment protocol and conditions. The shake tubes were incubated at 27˚C at a distance of 35 cm from the incandescent white light bulb. Colonies that formed after one month were transferred from the solid medium into the liquid medium that contained the same concentrations of $MnCl_2$ and Na_2S. Biofilms that grew in liquid after one month were mechanically dispersed by a syringe, inoculated into another set of agar shake tubes and incubated for one month. Colonies from the shake tubes were inoculated again into the liquid medium. The purity of the cultures at each transfer was tested by Sanger sequencing. Amplified 16S rRNA genes were sequenced in both directions using either 27F (5'- AGAGTTTGATCCTGGCTCAG-3') or 1492R (5'-ACG GCT ACC TTG TTA CGA CTT-3') (IDT Integrated DNA Technologies, Inc., Coralville, IA, USA), assembled to get a nearly full-length 16S rRNA gene (GeneWiz, Madison, WI, USA) and identified using nucleotide BLAST on GeneBank[37]. Future experiments should also explore the possibility of light-dependent production of organoperoxides in the medium as a function of vitamins and Fe(II) in the medium.

1.3. DNA extraction, 16S rRNA gene Illumina sequencing and phylogenetic analyses

A 500 µl sample of each biofilm enrichment (including early enrichments and the lake inoculum) was harvested and spun down into a pellet. Total DNA was extracted from samples using the PowerSoil® DNA Isolation Kit (MoBio, Carlsbad, CA, USA) according to manufacturer's instructions and eluted in 60 µl C6 solution. Upon extraction, DNA was quantified using NanoDrop (Thermo Scientific, Inc., Wilmington, DE, USA). The extracted samples and blank-template controls from the PowerSoil DNA Isolation kit were stored at -80˚C and sent to Argonne National Lab (Lemont, IL, USA) on dry ice for sequencing. The community composition was characterized using 16S rRNA gene amplicon paired-end sequencing on the MiSeq Illumina platform. Briefly, V4 region of the 16S rRNA gene (515F-806R) from each sample was amplified using the bacterial-specific primers 515F (5'-GTGCCAGCMGCCGCGGTAA-3') and 806 R (5'-GGACTACHVGGGTWTCTAAT-3') using PCR conditions[38]. After the amplifications, the PCR amplicons were quantified using Quant-iT PicoGreen dsDNA Assay Kit (ThermoFisher/ Invitrogen cat. no. P11496) according to manufacturer's instructions and pooled in equal concentrations (240 ng) to a single tube. This pool was cleaned up using MoBio UltraClean PCR Clean-Up Kit (MoBio, Carlsbad, CA, USA) and quantified using the Qubit (Invitrogen, Carlsbad, CA, USA). The pooled samples were sequenced on the Illumina MiSeq platform (Illumina, San Diego, CA, USA). All library preparations, pooling, quality controls and sequencing runs were performed at the Argonne National Lab (Lemont, IL, USA). Sequence data were analyzed using QIIME v.1.9.0[39]. Paired-end reads were joined using fastq-join method[40], and libraries were demultiplexed and filtered.

Any reads that did not assemble by perfect matches in the overlapping region or meet the q-score (>20) threshold were removed and were not used in subsequent analyses. Chimeric sequences were identified using UCHIME's usearch61 *de novo* based chimera detection algorithm[41] and removed from the quality-filtered sequences. Filtered and chimera-free sequences were aligned and clustered into operational taxonomic units (OTUs) at >97% similarity level using closed-reference UCLUST algorithm against the Greengenes v13.8 reference dataset as a database[42]. The most abundant sequence from each cluster was selected as a representative sequence. All representative sequences were aligned using PyNAST[39]. A phylogenic tree for subsequent phylogenetic analyses was built using FastTree[43]. OTU counts were rarified to 10,000 sequences per sample for diversity analysis using taxonomic and phylogenetic indices that included the Shannon and Faith's PD index. To identify bacterial taxa whose sequences are more abundant in samples grown in light and/or with Mn(II), we used LEfSe which performs a nonparametric Wilcoxon sum-rank test followed by linear discriminant analysis (LDA) coupled with effect size measurements to assess differentially abundant taxa[44]. Chlorobium sequences were significantly enriched in samples grown in the presence of light and Mn(II) with LDA score >5. Cultures grown in light had significantly more *Chlorobium* sp. (ANOVA, $F = 23.4521$, df factor = 5, df error = 12, $p < 0.0001$; Tukey's HSD, $p < 0.01$). Sequence data are available as FASTQ files at the National Center for Biotechnology Information (NCBI) via Sequence Read Archive (SRA), under the SRA accession ID number SRP133329.

1.4. Metagenome sequencing and analysis

To determine the metabolic potential of cultures grown from colonies that targeted specific growth conditions (see Section 1.2), we sequenced their metagenomes. The DNA of enrichments obtained using Condition 1 was extracted using a modified phenol-chloroform method with ethanol precipitation previously described[45] and quantified by a Qubit 2.0 Fluorometer (Thermo Fisher Scientific, Chino, CA, USA). This DNA was sent for metagenomic sequencing to the University of Southern California's Genome and Cytometry Core Facility (Los Angeles, CA, USA). The library preparation, quality control, and sequencing were performed at the Cytometry Core Facility. Briefly, before sequencing on Illumina HiSeq 2500 platform, DNA was sheared using dsDNA Shearas Plus (Zymo, Irvine, CA, USA), cleaned up using Agencourt AMPure XP beads (Beckman-Coulter, Indianapolis, IN, USA), the library was quantified using the Qubit 2.0 Fluorometer and the DNA fragment size was determined with an Agilent Bioanalyzer 2100.

The quality control of the sequence data was performed using Trimmomatic v0.36 using default parameters and a minimum sequence length of 36 bp[46]. IDBA-UD v1.1.2. was used to assemble the reads with a 2000 bp minimum contig length. SAMtools v.1.3.1[47] was used to convert files to binary format for downstream analysis. VizBin was used to delineate individual genomes from the enrichment metadata[48] and the genomes were assigned putative taxonomic identities according to their placement in a phylogenetic tree in CheckM v.1.0.4 using the "tree" command[49].

Individual genomes obtained from the metagenome data were submitted to the DOE Joint Genome IMG-MER (Integrated Microbial Genomes) pipeline for gene calling and assembly[50]. Protein-coding gene-prediction tool Prodigal v.3.0.0 was used to determine genes in the enrichment grown from the colony on 1 mM $MnCl_2$ and 20-50 μM Na_2S. The genome of *C. limicola* was 98.4% similar to *Chlorobium limicola* Frassasi[51].

To detect putative Mn(II)-oxidizing genes in *Chlorobium limicola*, we first generated a blast database of protein-coding Mn(II)-oxidizing genes by selecting genes encoding for multi-copper oxidases (MCOs) and animal heme peroxidases (AHPs). Because MCOs and AHPs each contain several classes of enzymes and can transfer electrons from a number of different substrates, we focused on enzymes with confirmed manganese-oxidizing activities by biochemical and molecular assays. All MCOs and AHPs involved in Mn(II)-oxidation and characterized to date are from aerobic microorganisms and include genes such as *mnxG*, *mcoA*, and *mopA* in *Pseudomonas putida*[19], *mnxG* in the spores of *Bacillus* strain SG-1[18], *moxA* in *Pedomicrobium* sp. ACM 3067[52], *mopA* in *Aurantimonas manganoxydans* SI85-9A1[53], and *Roseobacter sp.* AzwK-3b[20]. To determine whether *Chlorobium* has any homologs with characterized manganese-oxidizing MCOs and AHPs, we used BLASTp[54] and queried translated Mn(II)-oxidizing genes against the *Chlorobium* genome with an e-value cutoff of 10^{-5} and a bit score of 30. Homologs of MCOs and AFPs in *C. limicola* are shown in Extended Data Table 4.

Sequence data for *C. limicola* can be accessed at the JGI-IMG under IMG Submission ID 124328.

2. Spectroscopy

2.1. X-ray photoelectron spectroscopy

X-ray photoelectron spectroscopy was performed on a K-alpha™ + X-ray photoelectron spectrometer (XPS, K-Alpha + XPS, Thermo Fisher, MA, USA). Biofilms were harvested and centrifuged at 14,000 rpm for 5 min in the anaerobic chamber to form pellets. The pellets were placed on double-sided carbon tape and dried in the anaerobic chamber. To maintain the anoxic conditions, the samples were stored in the anaerobic chamber in hermetically sealed glass vials before analysis. All samples were fractured in high vacuum (3×10^{-8} Torr) in the Kratos outer pressure chamber and then moved directly into the main XPS measurement chamber. An incident monochromatic X-ray beam from the Al K Alpha target (15 kV, 10 mA) was focused on a 0.4 mm × 0.3 mm area of the surface at a 45° angle with respect to the sample surface. Depth profile etching with an etch cycle of 30 s and a total of 10 levels yielded high resolution spectra. The electron energy analyzer perpendicular to the sample surface was operated with a pass energy of 50 eV to obtain XPS spectra at a 0.1 eV step size and a dwell time of 50 ms. Each peak was scanned 15 times. To ensure representative data from heterogeneous samples, we probed a total of 50-80 points per sample. XPS data were treated and analyzed using CasaXPS curve resolution software package. Spectra were best fit after Shirley background subtractions by non-linear least squares CasaXPS curve resolution software package. Gaussian/Lorentzian (G/L) contributions to the line shapes were numerically convoluted using a Voigt function. The different XPS lines with sets of Gaussian and Lorentzian peaks were empirically fitted with different standards corresponding to different oxidation sets (MnO, $MnCO_3$, Mn_2O_3, Mn_3O_4, MnO_2, $MnCaO_3$). Each Mn XPS spectrum was empirically best fitted with multiple standard phases (MnO, $MnCO_3$, Mn_2O_3, Mn_4O_3, MnO_2, $MnCaO_3$) that produced the minimum residual. The average fit properties for all treated spectra were acceptable as the following: R expected= 1.60, R profile= 1.71, significance level= 0.05, residual standard deviation= 1.67, goodness of fit= 1.78, critical Chi-square= 3.84.

2.2. Interpretation of XPS spectra

The redox state of manganese in microbial cultures was confirmed by XPS (Extended Data Fig. 3). The Mn2p XPS spectra of the dark culture exhibited two major peaks at binding energies of 640.90 eV and 652.2 eV corresponding to $Mn2p_{2/3}$ and $Mn2p_{1/2}$, respectively. This is in agreement with other reports on Mn(II) phases of Mn[55,56]. In the photosynthesizing culture, the Mn2p peak shifted to a high-energy side and the intense satellite peak characteristic of Mn(II) diminished. These biofilms contained Mn in different valence states. At some analyzed spots, the Mn2p XPS spectrum exhibited two major peaks of $Mn2p_{2/3}$ and $Mn2p_{1/2}$ at binding energies of 642 eV and 653 eV, respectively. These correspond to Mn(IV) in calcium-manganese oxide phases[57]. Peaks at $Mn2p_{2/3}$ with binding energies 641.61 eV and 641.47 eV, respectively, were also detected. These peaks correspond to Mn(III) in Mn_2O_3 and Mn(III) and Mn(II) in Mn_3O_4 phases[58,59].

The redox state of the manganese in the culture enriched in condition 1 and condition 2 was confirmed by XPS (Extended Data Fig. 8). The Mn2p XPS spectra of this culture (Extended Data Fig. 8a) exhibited two major peaks at binding energies of 641.41 eV and 653.15 eV corresponding to $Mn2p_{2/3}$ and $Mn2p_{1/2}$, respectively and matching Mn_3O_4[58]. The Mn2p XPS spectra of Condition 2 enrichment (Extended Data Fig. 8b) exhibited $Mn2p_{2/3}$ peaks at 640.97 eV and 652.2 eV corresponding to $Mn2p_{2/3}$ and $Mn2p_{1/2}$ respectively. This is in agreement with other reports of MnO phase[60].

2.3. Probing the redox state of manganese in biofilms

We used X-ray Photoelectron Spectroscopy (XPS) to detect oxidized manganese in colonies enriched on 1 mM Mn(II) (Condition 1). Table 3 in Extended Data summarizes the procedure used to study the Mn(II) oxidation activity in the enrichment cultures. Manganese oxidation was tested using cultures that were enriched as colonies in agar shake tubes (Condition 1, Condition 2, Section 2, Table 3 in Extended Data). Biofilms from condition 1 were grown in duplicate 10 ml cultures with 1 mM $MnCl_2$ and 0.02 mM Na_2S, mechanically dispersed and resuspended into separate 10 ml liquid solutions. Five percent v/v of this suspension was transferred into 10 ml of MFGL medium with 1 mM $MnCl_2$ and 0.02 mM Na_2S and the cultures were incubated at 27 $^{\circ}$C for one week before the assay. A second assay tested the Mn(II) oxidation activity without requiring the very sparse biofilm to grow. Condition 1 enrichment was grown for two weeks as described above, centrifuged at 8000 rpm in the anaerobic chamber, washed 3 times with anaerobic water and transferred into 10 ml of MFGL with 1 mM $MnCl_2$ and 0.02 mM Na_2S. These cultures were incubated for 3 days in a 12 h/12 h light/dark regime and harvested anaerobically. This procedure preserved the cell density of the original biofilms and did not require microbial growth.

To test for Mn (II) oxidizing activity in the enrichment from condition 2 (*Chlorobium* sp. and *Desulfomicrobium* sp.), the culture was grown in 10 ml of the basal MFGL amended with 1 mM Na_2S, harvested anaerobically, and dispersed in 10 ml of the basal MFGL medium. This suspension was used to inoculate 10 ml of the basal MFGL amended with 1 mM $MnCl_2$ and 0.02 mM Na_2S at 5% v/v. The inoculated medium was incubated in the light/dark regime for one week. To test for Mn(II) oxidizing activity without requiring the low-biomass biofilms to grow, the enrichment from condition 2 was grown for two weeks in 10 ml of the basal MFGL amended with 1 mM Na_2S, centrifuged at 8000 rpm in the anaerobic chamber, washed 3 times with anaerobic water and transferred to 10 ml of MFGL with 1 mM $MnCl_2$ and 0.02 mM Na_2S. These cultures were incubated for three days in the 12h/12h light/dark regime and harvested anaerobically. All collected microbial pellets were dried on carbon tape and stored anaerobically

inside serum bottles with N_2 atmosphere and placed inside the anaerobic chamber in the dark at 26 °C until XPS analysis.

2.3.1. Probing the redox state of manganese in co-cultures

Chlorobium limicola (DSM 245, DSMZ GmbH Germany) and *Chlorobium tepidum* (DSM 12025, DSMZ GmbH, Germany) were inoculated with 5% v/v inoculum and grown in 50 ml MFGL medium supplemented with 0.05 mM Na_2S and 0.5 g/L yeast extract in a 12 h/12 h light/ dark regime at 27 °C for 3 weeks. *Geobacter lovleyi* (DSM 17278, DSMZ GmbH Germany) was grown in MFGL supplemented with 2.8 mM ferrihydrite and 5 mM acetate and reduced with 0.05 mM Na_2S in the dark at 21 °C for 3 weeks. Microbes from these cultures were inoculated as 5% v/v inoculum in the following combinations: *C. limicola* + *C. tepidum, C. tepidum* + *G. lovleyi, C. limicola* + *G. lovleyi, C. limicola* + *C. tepidum* + *G. lovleyi*. All these co-cultures were grown in 10 ml MFGL medium with 1 mM Mn(II) and 0.05 mM Na_2S in a 12 h/12 h light/ dark regime at 27 °C for 2 weeks. The biomass was harvested anaerobically, the pellets were dried on carbon tape and stored anaerobically under N_2 inside the anaerobic chamber in the dark at 26 °C until XPS analysis. The oxidation state of Mn was characterized by XPS in all four cultures.

3. X-ray powder diffraction

X-ray powder diffraction (XRD) patterns were obtained in reflection mode with Ni-filtered Cu Kα radiation (λ= 1.5406 Å) as X-ray source on an X'Pert PRO diffractometer (XRD, X'Pert PRO, PANalytical, Netherlands) equipped with an X'Celerator detector (PANalytical, Netherlands). The patterns were measured in 2θ range from 3° to 90° with a scanning step of 0.008° and a fixed counting time of 600 s at 45 kV and 40 mA. Biofilms were harvested and centrifuged at 14,000 rpm for 5 min in the anaerobic chamber. Microbial paste was smeared on Zero Diffraction Disk (23.6 mm diameter x 2.0 mm thickness, Si crystal, MTI corporation, CA, USA) and dried in the anaerobic chamber. The samples were analyzed inside the anaerobic dome to maintain the anoxic conditions during the XRD analyses. Data were analyzed and fitted using High Score Plus program version 4.5. The average fit properties for all treated spectra were acceptable as the following: Residual Standard Deviation= 1.63, R expected= 1.28, R profile= 1.63, Significance level= 0.05, Goodness of Fit = 1.69, Critical Chi-square = 3.84.

Precipitated minerals were also analyzed using in-situ synchrotron-based X-ray diffraction (SR-XRD) at the Advanced Light Source (ALS) at the beamline 12.3.2. Biofilms were harvested on site and the biofilm paste was loaded into transmission sample XRD cells. The transmission synchrotron diffraction data were collected using a DECTRIS Pilatus 1M hybrid pixel area detector placed at an angle 2θ of 35° at approximately 170 mm from the sample. The 4-bounce monochromator was set to an energy was 10 keV (λ = 1.239842 Å). The sample geometry with respect to the incident beam and the detector was carefully calibrated using Al_2O_3 powder. The 2D diffraction patterns (Fig.1d) were analyzed and integrated along the azimuthal direction into 1D diffractograms using the X-ray microdiffraction analysis software (XMAS v6) developed at the Advanced Light Source for the ALS beamline 12.3.2 and Matlab R2017a.

3.1. Determination of XRD detection limit

To determine the detection limit of XRD, 0.05, 0.01, 0.02, and 1 mg of MnO_2 was mixed with 10 mg of dry anaerobic biofilm that did not contain green sulfur bacteria or manganese oxides and spread on Zero Diffraction Disk (23.6 mm diameter x 2.0 mm thickness, Si crystal, MTI corporation, CA, USA). The mixtures were analyzed by X'Pert PRO diffractometer XRD, X'Pert PRO, PANalytical, Netherlands) equipped with an X'Celerator detector (PANalytical, Netherlands) over 10-hour analysis time. MnO_2 standard and the bacterial biofilm were also run separately as controls. The detection limit of XRD was determined by the mass of MnO_2 that yielded discernible diffraction peaks in the XRD spectrum.

3.2. Interpretation of XRD peaks

The XRD spectra of microbial cultures incubated in the light with Mn(II) (Fig. 2) showed peaks that can be indexed to a ternary manganese oxide; $CaMnO_3$ (ICDD-01-016-2217) with lattice constants of a= 5.2917 nm, b= 7.4803 nm and c= 5.2870 nm[61]. $CaMnO_3$ is not known to occur naturally.

Dolomite was the most abundant phase in the cultures and its peaks were indexed as (104), (101), (110), (11-3), (202) and (018) (ICDD-04-011-9833). The absence of light inhibited the growth of photosynthetic microbes and the formation of manganese oxide minerals and also reduced the precipitation of dolomite (Fig. 2). Biofilm incubated in the dark showed the precipitation of calcium carbonate phase, $CaCO_3$ (ICDD-00-058-0471) indexed for (121) and (102). In addition to the various carbonate phases, the XRD spectrum showed two different phases of sulfur (S°); (ICDD-04-020-2294) indexed for (110), (-101) and (-211) and (ICDD-05-001-0219) indexed for (110) and (-101).

The XRD spectra of microbial cultures incubated at different concentrations of Mn and S showed peaks of manganese oxide, dolomite and elemental sulfur (Extended Data Fig. 5). The latter formed in microbial cultures incubated at high concentrations of H_2S (0.25-1 mM) and in the cultures grown with less than 1 μM Mn(II) (Extended Data Fig. 6; see trace metal solution composition in Section 1.1.). Elemental sulfur, S° (ICDD-05-001-0219), was indexed for (110), (-101), (011) and (-211).

Extended data Fig. 10 shows two XRD spectra of microbial cultures incubated in the light. The top spectrum is the analysis of microbial biofilms without treatment showing peaks of manganese oxide, $CaMnO_3$ (ICDD-01-016-2217) and dolomite, $CaMg(CO_3)_2$ (ICDD-04-011-9833). The bottom spectrum is the analysis of treated microbial biofilms showing only peaks of elemental sulfur S° (ICDD-05-001-0219) and a calcium carbonate phase, $CaCO_3$ (ICDD-00-058-0471).

4. Microscopy

4.1. Scanning electron microscopy

Scanning electron micrographs were acquired by a Zeiss Merlin scanning electron microscope with the GEMINI II column (SEM, Zeiss Merlin SEM, Carl Zeiss microscopy, CA, USA). The microscope was equipped with a field gun emission and energy dispersive X-ray spectrometer (EDS, EDAX detector; EDAX, NJ, USA) that operated at an accelerating voltage of 5 - 15 kV, probe current of 100 pA, and a working distance of 8.5 mm. On-axis in-lens secondary electron (SE-mode) detector was used during imaging. The samples were fixed by 0.2 M sodium cacodylate, 0.1% $CaCl_2$ and 2.5% glutaraldehyde in anaerobic water for 2-3 days at 4°C. The

fixed samples were washed by 0.1 M sodium cacodylate followed by a wash in nanopure water. After washing, the samples were dehydrated with a series of ethanol-water solutions. The ethanol-water solution series included the following dehydration steps: 30% (20 min), 50% (20 min), 70% (20 min), 80% (20 min), 90% (20 min) and 100% (3×20min) of 200 proof ethanol. After air-drying, the samples were mounted on double-sided carbon tape and coated with a thin layer 5 nm of Au/Pd or 10 nm of carbon using a Hummer V sputter coater. EDS spectra were treated and analyzed by TEAM EDS 2.0 analysis software (EDAX, NJ, USA) and Microsoft Excel 2016.

4.2. Transmission electron microscopy

Transmission electron micrographs were obtained using FEI Tecnai F20 supertwin microscope (TEM, FEI Tecnai G2, FEI, OR, USA) with a 200 kV Schottky field emission gun. The samples were imaged at 80 kV with 1024 × 1024 CCD Gatan camera (Gatan, CA, USA). The samples were fixed by 0.2 M sodium cacodylate, 0.1% $CaCl_2.6H_2O$ and 2.5% glutaraldehyde in aerobic nanopure water for 2-3 days at 4°C. The samples were then washed with washing buffer (0.1 M sodium cacodylate in nanopure water), postfixed with 1% osmium tetroxide in water for 1 hour, washed with aerobic nanopure water, and stained with 1% uranyl acetate for 1 hour. The stained samples were washed with nanopure water and dehydrated with a series ethanol-water solution. The ethanol-water solution series included the following dehydration steps: 30% (20 min), 50% (20 min), 70% (20 min), 80% (20 min), 90% (20 min), and 100% (3×20 min) of 200 proof ethanol. The samples were further dehydrated with propylene oxide:ethanol solvent (50:50, by vol) for 30 min, then with 100% propylene oxide. The epoxy resin used for embedding consisted of diglycerol ether of polypropylene glycol (EmBed 812, DER 736, Electron Microscopy Sciences, EMS #14130, PA, USA), cycloaliphatic epoxide resin (ERL 4221 Electron Microscopy Sciences, EMS #14300, PA, USA), Nonenyl succinic anhydride (NSA, Electron Microscopy Sciences, EMS#14300, PA, USA) and 2-(dimethylamino)ethanol (DMAE, Electron Microscopy Sciences, EMS#14300, PA, USA). The samples were embedded in resin and cut into 80 nm thick sections with a diamond knife using Leica Reichert Ultracut E microtome (Reichert Ultracut E microtome, Leica, Germany) with a thickness setting of 50 nm. Thin sections were placed on FCF-200 grids (Electron Microscopy Sciences, Cat# FCF-200-Cu, PA, USA).

To determine whether the fixation and embedding protocols introduced any artifacts, photosynthetic biofilms were also harvested without any further processing or staining in the anaerobic chamber. A drop of microbial culture was deposited on LC-200 grid (Electron Microscopy Sciences, Cat#LC-200-Cu, PA, USA) and imaged with JEOL 2010F transmission electron microscope (TEM, JOEL 2010F, JOEL, CA, USA). The JEOL 2010F TEM is equipped with a Schottky field emission gun (FEG) operating at 200 kV and a Gatan energy filter (GIF, Gatan 200, Gatan, CA, USA). The 2010F TEM has micro-diffraction, diffraction pattern in parallel beam, and convergent beam electron diffraction features to allow selected area electron diffraction (SAED) on selected mineral-encrusted bacteria with a high spatial resolution. Gold standard was used as reference for SAED analyses. The high-angle annular dark filed detector (HAADF, Gatan, CA, USA) for atomic resolution scanning electron transmission microscopy in the free-lens control mode (STEM) and with an energy dispersive spectrometer (EDS, Bruker silicon drift detector SDD, Bruker, MA, USA) enabled elemental analysis at nanoscale resolution**.** Images in the TEM and STEM mode were taken by a digital camera (Gatan Orius,

Gatan, CA, USA). SAED patterns were imaged using Gatan digiscan unit (Gatan, CA, USA). TEM, STEM and SAED images were recorded and treated using Gatan digital micrograph software (Gatan, CA, USA). EDS spectra were recorded and treated using INCA program (Oxford instruments, UK).

4.3. Interpretation of SAED patterns

Different types of manganese minerals in photosynthetic biofilms corresponded to different stages of mineral maturation. HRTEM of the manganese oxide nanocluster surrounding a cell (Fig. 3) showed polycrystalline minerals with a uniform lattice fringe that corresponded to the (116) plane with interplanar spacing of 2.71 Å of calcium manganese oxide (ICDD-00-053-0092). The SAED patterns of minerals that were not associated with cell surfaces showed various minerals. One type of manganese mineral had four obvious polycrystalline diffraction rings that could be observed at 3.65 Å, 3.40 Å, 2.88 Å and 1.83 Å, respectively. These corresponded, respectively, to the (112), (211), (220) and the (323) crystal planes of Mn_3O_4 (ICDD-03-065-2776) (Fig. 3). Some globular nanocrystals of manganese oxide outside of any microbial surfaces (Fig. 3) showed lattice fringes with the interplanar spacing of 2.26 Å. This matched the characteristic interplanar spacing of the (200) plane of manganese oxide type MnO mineral (ICDD-04-004-3858).

5. Concentrations of dissolved species in culture media

Sulfide concentrations were determined by the modified method of Cline[62] in samples of triplicate cultures for each time point. Briefly, 200 µL of each liquid sample was diluted in 1 ml of 0.05 M zinc acetate. Standards were prepared from 1 mM anaerobic stock solution of Na_2S diluted by 0.05 M zinc acetate. The concentration of Na_2S stock solution was verified by precipitating an exact volume of Na_2S with an excess volume of 0.3 M silver nitrate. 600 µL of the precipitated sample were transferred and reacted with 10 µL of diamine reagent. After 20 minutes reaction time in the dark, the absorbance was measured by a multi-mode reader spectrophotometer (BioTek, Synergy 2, Winooski, VT, USA) at 670 nm.

The concentrations of sulfate, nitrite and nitrate in the samples of the liquid medium from triplicate cultures were determined by ion chromatography (IC, Dionex ICS-16000 equipped with an auto-sampler Dionex AS-DV, ThermoFisher, USA), guard column (Dionex Ion Pac™AG22, RFIC™, Guard 2x50 mm, Thermo Fisher, USA), analytical column (Dionex Ion Pac™ AS22, RFIC™, Analytical 2X250mm, Thermo Fisher, USA) and a trap column for metals (Dionex Ion Pac™ MFC-1, RFIC™, trap column, metal free, 3x27mm, Thermo Fisher, USA). All samples were filtered anaerobically through 0.2 µm pore-size filters (Acrodisc 25 mm syringe filter, PALL corporation, MA, USA) and stored at -20 °C. Chloride ion was solid-phase extracted from all samples using a Ag/H cartridge (Dionex OnGuard™ II Ag/H, 2.5 cc cartridge, Thermo Fisher, USA) before the analysis. The removal of chloride ion affected the lower detection limit for phosphate, but not for sulfate and nitrate. The limits of detection for sulfate, nitrate and nitrite, respectively, were 20 µg/L, 20 µg/L and 10 µg/L respectively.

Total dissolved manganese concentrations in the liquid culture media from triplicate cultures were determined by inductively coupled plasma-mass spectrometry (ICP-MS, Agilent 7500, Agilent, USA). All samples were filtered through 0.2 µm pore-size filters (Acrodisc 25 mm syringe filter, PALL corporation, MA, USA), and acidified with 2% high purity HCl (hydrochloric acid 30%, Sigma Aldrich, suprapur- end Millipore, 100318, MO, USA) and stored

at -20 °C. All samples were diluted with high purity 2% HCl (hydrochloric acid 30%, Sigma Aldrich, suprapur- EMD Millipore, 100318, MO, USA) before the analysis. These measurements did not reveal any oxidized manganese in the liquid phase.

Dissolved manganese in the liquid phase was also measured by leucoberbelin blue (LBB) assay[63] and iodometric method[64]. Oxidized manganese in the liquid phase includes any soluble valence state of Mn that can be filtered through the 0.2 μm pore filter. We used the iodometric method[64,65] to determine Mn oxidation state including Mn(II), Mn(III), Mn(IV) and Mn(VII). Again, none of the measurements detected oxidized manganese in the liquid phase. LBB assay was also used to quantify the concentrations of oxidized manganese in biofilms. These concentrations were detected as oxidizing equivalents of $KMnO_4$ (Section 6).

The concentration of peroxide was measured in triplicate samples of microbial biofilms and sterile controls incubated in the light with 1 mM Mn(II) and 50 μM Na_2S using a peroxidase activity assay kit (Sigma Aldrich, MAK092, MO, USA). The standard curve was measured using different dilutions of the H_2O_2 standard (Sigma Aldrich, MAK092C, MO, USA) in sterile culture medium mixed with the reaction mix composed of 2 μL fluorescent peroxidase substrate (Sigma Aldrich, MAK092B, MO, USA) and 48 μL of HRP positive control (Sigma Aldrich, MAK092D, MO, USA). A 100 μL of each diluted H_2O_2 standard and the samples were distributed into microplate wells. The plate was incubated at 37°C and the initial measurement ($T_{initial}$) was measured after 3 minutes by multi-mode reader spectrophotometer (BioTek, synergy 2, Winooski, VT, USA) at 570 nm. The absorbance was measured every 3 minutes until the value of the most active sample exceeded the end linear range of the standard curve. We did not detect any H_2O_2 in the incubations or sterile controls. The limit of detection of H_2O_2 using colorimetric detection was 0.1 nM.

6. Quantification of biofilms and oxidized manganese in biofilms

The amount of biofilm was measured by crystal violet (CV) staining using the modified assay of O'Toole[66]. Briefly, biofilms from triplicate serum bottles were harvested at each time point and centrifuged aerobically at 10,000 rpm for 30 minutes. The supernatant was decanted and 0.5 ml of 0.1% of aqueous crystal violet added (crystal violet, Sigma Aldrich, ACS reagent, ≥ 90 % anhydrous basis, C6158, MO, USA). The stained biofilm was incubated in the dark at room temperature for 24 hours, washed 15 times with nanopure water, and air-dried. After drying, 0.5 ml of 30% acetic acid (37 % Acetic acid, Sigma Aldrich, ACS reagent, ≥ 99.7%, 695092, MO, USA) was added to the samples and left to react at room temperature for 30 minutes. Acetic acid solubilized all crystal violet molecules bound to peptidoglycan and exopolysaccharide. Thus, the solubilized CV corresponds to the biomass in biofilms. The collected solubilized CV was filtered through 0.2 μm pore-size filters (Acrodisc 25 mm syringe filter, PALL corporation, MA, USA) and 200 μl of the solution was transferred into a microtiter plate. The absorbance of the samples was measured at 550 nm using a spectrophotometer (BioTek, synergy 2, Winooski, VT, USA).

Oxidized manganese in biofilms was quantified by the leucoberbelin blue assay (LBB). Biofilms were inoculated from frozen stocks into triplicate serum bottles that contained 25 ml or 50 ml of MFGL medium and incubated for one-, two or three weeks. Biofilms from the frozen stock (~ 5 mg) were washed 10 times with anaerobic nanopure water to remove any glycerol, inoculated into the culture medium and the medium was immediately flushed with 20 % CO_2/80 % N_2 (v/v) for 1 hour. The biofilms grew for two weeks in the light, at which point, biofilms (~ 5

mg) were transferred into serum bottles that each contained 25 ml of the fresh MFGL medium. Three bottles were incubated in the light, three in the dark and all biofilms were harvested after one or two weeks by pipetting and centrifugation in the anaerobic glove box. After the LBB assay, all analyzed samples were air-dried for > 24 h and weighed. The one-week old biofilms weighed 16-18 mg, the two-week old biofilms weighed 19-21 mg. A separate experiment quantified the amount of oxidized manganese in duplicate 25 ml cultures of three-week old biofilms that had been inoculated with ~ 0.1 mg of the washed material from frozen culture stocks and weighed <0.3 mg at the end of the experiment. In contrast to the experiments that yielded samples for XRD, XPS, SEM and TEM analyses, these experiments involved at most one successive transfer of biofilms after the inoculation from frozen stocks of biofilms enriched as described in Section 1.1.

The working reagent was prepared as 0.04% LBB in 45 mM acetic acid and stored at 4°C overnight in a light-proof container. Potassium permanganate ($KMnO_4$) 1 mM stock solution was freshly prepared in water and standards (5, 10, 15, 20, 40, 50 μM) were prepared by diluting the stock solution in water. The samples were incubated for 20 minutes in 0.75 ml of the 0.04% LBB working reagent in the dark at room temperature and centrifuged for 90 s at 10,000 rcf to remove the biofilm and mineral particulates from the solution. The absorbance of the supernatant was measured on a spectrophotometer at 618 nm. To determine whether some manganese was oxidized in the dark, ~ 5 mg of the biofilm stock was inoculated into sterile MFGL in the dark for two weeks which detected on average 0.02 μM oxidizing equivalent per 5 mg of biofilm. Control experiments assayed the concentration of oxidized manganese in FGL enrichment cultures that contained 1 mM sulfide and 1 mM $MnCl_2$ and did not detect any.

7. Oxygen concentration

To determine how much oxygen can diffuse into the cultures through the butyl rubber caps, we used our in-house developed oxygen sensor[67], based on the fluorescence lifetime of 5,10,15,20-tetrakis(pentafluorophenyl)-21H,23H-porphine palladium(II)[68]. The sensor can detect changes in the partial pressure of oxygen that are smaller than 1 μbar and its main sensitivity region is 0-100 μatm[67].

Experiments were conducted to quantify the oxygen concentration in the cultures and the maximum amount of oxygen inflow. First, the partial pressures of oxygen in the headspaces of photosynthetic cultures, sterile controls incubated in the light, and dark control cultures were measured automatically for 14 days. All serum bottles contained 100 mL of the medium reduced by 50 μM Na_2S (Extended Data Figure 1). The partial pressure of oxygen in the headspaces of the bottles did not increase or fluctuate by more than 2 μbar over the course of the growth experiment. The main sources of noise were daily thermal fluctuations (high frequency component) and sensor aging (low frequency component). The upper limit for the partial pressure of oxygen in the headspace is 2 μbar, measured in the beginning of the experiment. This partial pressure was lower than 0.5 μbar during most of the experiment. This corresponds to a maximum dissolved molecular oxygen concentration of 2.6 nM, assuming the equilibrium between O_2 in the headspace and O_2 dissolved in the culture medium according to Henry's law.

In an additional test, we incubated biofilms in the light in the anaerobic chamber under a 5%CO_2: 5%H_2: balN_2 (v/v/v) atmosphere. The partial pressure of oxygen in the chamber was below 1 ppm, as opposed to 21% above the butyl rubber stoppers of the cultures that were

incubated outside of the chamber. Therefore, orders of magnitude less oxygen is expected to diffuse into the cultures. The biofilms were grown with and without the addition of 1 mM Mn(II) and the culture medium was reduced with 20 μM Na_2S. After two weeks of incubation, the biofilms were harvested and analyzed by XRD. Manganese oxides and carbonates phases formed in biofilms incubated with Mn(II), elemental sulfur formed in biofilms grown without Mn(II). The formation of detectable quantities of manganese oxides in photosynthetic cultures incubated in the anaerobic glove box further demonstrated the negligible role of oxygen diffusion in the oxidation of manganese.

8. Acquisition of phototrophy in green sulfur bacteria

Phototrophy within stem group green sulfur bacteria (GSB) and stem group green non-sulfur bacteria (GNS) could have been acquired at any point before their post-GOE diversification events. Without additional information, it is not possible to infer where along these branches phototrophy was acquired, but the evolutionary history of bacteriochlorophyll biosynthesis may provide a strong clue. Phylogenies of protein families involved in bacteriochlorophyll biosynthesis have a complex evolutionary history across phototrophic lineages, including gene duplications within stem GSB, and multiple HGT events between GSB and GNS lineages[69]. Specifically, the genes encoding BchH and BchM were transferred from within crown GNS to stem GSB, with the gene encoding BchH undergoing a duplication shortly before crown GSB. BchI is also observed to duplicate in the GSB stem, with one paralog being transferred to stem GNS. These observations indicate that phototrophy must have existed in these lineages at the time of any bacteriochlorophyll synthesis gene duplications, or any divergence of an HGT donor lineage. A substantial history of phototrophy within the GSB stem lineage can be inferred from these events (Extended Data Fig. 13). Future molecular clock studies including these gene tree histories may be able to constrain the time interval for phototrophy in the GSB stem; but the Bch protein histories alone suggest that phototrophy within GSB existed much before the appearance of the GSB or GNS crown groups.

References

30 Bekker, A. *et al.* Dating the rise of atmospheric oxygen. *Nature* **427**, 117–120 (2004).

31 Balch, W. E. & Wolfe, R. S. New approach to the cultivation of methanogenic bacteria: 2-mercaptoethanesulfonic acid (HS-CoM)-dependent growth of *Methanobacterium ruminantium* in a pressurized atmosphere. *Appl. Environ. Microbiol.* **32**, 781-791 (1976).

32 Sim, M. S., Bosak, T. & Ono, S. Large sulfur isotope fractionation does not require disproportionation. *Science* **333**, 74-77 (2011).

33 Sim, M. S., Ono, S., Donovan, K., Templer, S. P. & Bosak, T. Effect of electron donors on the fractionation of sulfur isotopes by a marine *Desulfovibrio sp*. *Geochim. Cosmochim. Acta.* **75**, 4244-4259 (2011).

34 Liang, J., Bai, Y., Men, Y. & Qu, J. Microbe–microbe interactions trigger Mn (II)-oxidizing gene expression. *The ISME journal* **11**, 67-77 (2017).

35 Ljungdahl, L. & Wiegel, J. Working with anaerobic bacteria. *Manual of Industrial Microbiology* p. 115-127 American Society for Microbiolgy. (1986).

36 Pfennig, N. *Rhodocyclus purpureus* gen. nov. and sp. nov., a ring-shaped, vitamin B12-requiring member of the family Rhodospirillaceae. *Int. J. Syst. Evol. Microbiol.* **28**, 283-288 (1978).
37 Benson, D. A. *et al.* GenBank. *Nucleic. Acids. Res.* **41**, D36-D42 (2013).
38 Caporaso, J. G. *et al.* Global patterns of 16S rRNA diversity at a depth of millions of sequences per sample. . *Proc. Natl. Acad. Sci.* **108**, 4516-4522 (2011).
39 Caporaso, J. G. *et al.* QIIME allows analysis of high-throughput community sequencing data. *Nat. Methods* **7**, 335-336 (2010).
40 Aronesty, E. Comparison of sequencing utility programs. *Open Bioinformatics J.* **7**, 1-8 (2013).
41 Edgar, R. C., Haas, B. J., Clemente, J. C., Quince, C. & Knight, R. UCHIME improves sensitivity and speed of chimera detection. *Bioinformatics* **27**, 2194-2200 (2011).
42 McDonald, D. *et al.* An improved Greengenes taxonomy with explicit ranks for ecological and evolutionary analyses of bacteria and archaea. *ISME J* **6**, 610-618 (2012).
43 Price, M. N., Dehal, P. S. & Arkin, A. P. FastTree 2-approximately maximum-likelihood trees for large alignments. *PLoS One* **5**, e9490 (2010).
44 Segata, N., Izard, J., Waldron, L., Gevers, D., Miropolsky, L., Garrett, W. S., & Huttenhower, C. Metagenomic biomarker discovery and explanation. *Genome biology*, *12*(6), R60. (2011).
45 Momper, L. M., Reese, B. K., Carvalho, G., Lee, P. & Webb, E. A. A novel cohabitation between two diazotrophic cyanobacteria in the oligotrophic ocean. *ISME J* **9**, 882-893 (2015).
46 Bolger, A. M., Lohse, M. & Usadel, B. Trimmomatic: a flexible trimmer for Illumina sequence data. *Bioinformatics* **30**, 2114-2120 (2014).
47 Li, H. *et al.* The Sequence Alignment/Map format and SAMtools. *Bioinformatics* **25**, 2078-2079 (2009).
48 Laczny, C. C. *et al.* VizBin - an application for reference-independent visualization and human-augmented binning of metagenomic data. *Microbiome* **3**, 1 (2015).
49 Parks, D. H., Imelfort, M., Skennerton, C. T., Hugenholtz, P. & Tyson, G. W. CheckM: assessing the quality of microbial genomes recovered from isolates, single cells, and metagenomes. *Genome. Res.* **25**, 1043-1055 (2015).
50 Huntemann, M. *et al.* The standard operating procedure of the DOE-JGI Microbial Genome Annotation Pipeline (MGAP v.4). *Stand. Genomic. Sci.* **10**, 1-6 (2015).
51 Mansor, M., & Macalady, J. L. Draft genome sequence of lampenflora *Chlorobium limicola* strain Frasassi in a sulfidic cave system. *Genome announcements*, *4*(3), e00357-16. (2016).
52 Ridge, J. *et al.* A multicopper oxidase is essential for manganese oxidation and laccase-like activity in *Pedomicrobium* sp. ACM 3067. *Environ. Microbiol.* **9**, 944-953 (2007).
53 Anderson, C. R. *et al.* Mn (II) oxidation is catalyzed by heme peroxidases in *Aurantimonas manganoxydans* strain SI85-9A1 and *Erythrobacter* sp. strain SD-21. *Appl. Environ. Microbiol.* **75**, 4130-4138 (2009).
54 Altschul, S. F. *et al.* Gapped BLAST and PSI-BLAST: a new generation of protein database search programs. *Nucleic. Acids. Res.* **25**, 3389-3402 (1997).

55 Nesbitt, H. & Banerjee, D. Interpretation of XPS Mn (2p) spectra of Mn oxyhydroxides and constraints on the mechanism of MnO_2 precipitation. *Am. Mineral.* **83**, 305-315 (1998).
56 Oku, M., Hirokawa, K. & Ikeda, S. X-ray photoelectron spectroscopy of manganese—oxygen systems. *J. Electron. Spectrosc. Relat. Phenom.* **7**, 465-473 (1975).
57 Han, X., Zhang, J., Du, F., Cheng, J., Chen, J. Porous calcium–manganese oxide microspheres for electrocatalytic oxygen reduction with high activity. *Chem. Sci.* **4**, 368-376 (2013).
58 Audi, A. A. & Sherwood, P. M. A. Valence-band x-ray photoelectron spectroscopic studies of manganese and its oxides interpreted by cluster and band structure calculations. *Surf. Interface. Anal.* **33**, 274-282 (2002).
59 Toupin, M., Brousse, T. & Bélanger, D. Charge storage mechanism of MnO_2 electrode used in aqueous electrochemical capacitor. *Chem. Mater.* **16**, 3184-3190 (2004).
60 Foord, J., Jackman, R. & Allen, G. An X-ray photoelectron spectroscopic investigation of the oxidation of manganese. *Philos. Mag. A.* **49**, 657-663 (1984).
61 Božin, E. S. *et al.* Structure of $CaMnO_3$ in the range $10K \leqslant T \leqslant 550$ K from neutron time-of-flight total scattering. *J Phys Chem Solids* **69**, 2146-2150 (2008).
62 Cline, J. D. Spectrophotometric determination of hydrogen sulfide in natural waters. *Limnol. Oceanogr.* **14**, 454-458 (1969).
63 Krumbein WE, Altman HJ. A new method for the detection and enumeration of manganese-oxidizing and -reducing microorganisms. *Helgol Wiss Meeresunters* **25**:347–356 (1973).
64 Murray JW, Balistrieri LS, Paul B. The oxidation state of manganese in marine sediments and ferromanganese nodules. *Geochim. Cosmochim. Acta* **48**: 1237-1247 (1984).
65 Pierre Anschutz, Karine Dedieu, Franck Desmazes, Gwénaëlle Chaillou. Speciation, oxidation state, and reactivity of particulate manganese in marine sediments. *Chem. Geol.* **218**: 265-279 (2005).
66 Pajusalu, M., Borlina, C. S., Seager, S., Ono, S. & Bosak, T. Open-source sensor for measuring oxygen partial pressures below 100 microbars. *PLoS ONE* **13**, e0206678 (2018).
68 Lehner, P. *et al.* LUMOS--A sensitive and reliable optode system for measuring dissolved oxygen in the Nanomolar Range. *PLoS One* **10**, e0128125 (2015).
69 Sousa, F. L., Shavit-Grievink, L., Allen, J. F. & Martin, W. F. Chlorophyll biosynthesis gene evolution indicates photosystem gene duplication, not photosystem merger, at the origin of oxygenic photosynthesis. *Genome Biol. Evol.* **5**, 200–216 (2012).
70 Gibson, J. A. E. *et al.* Geochemistry of ice-covered, meromictic Lake A in the Canadian High Arctic. *Aquat. Geochem.* **8**, 97–119 (2002).
71 Green, W. J., Ferdelman, T. G. & Canfield, D. E. Metal dynamics in Lake Vanda (Wright Valley, Antarctica) *Chem. Geol.* **76**, 85-94 (1989).
72 Dickman, M. & Ouellet, M. Limnology of Garrow Lake, NWT, Canada. *Polar Rec* **23**, 531-549 (1987).
74 Gallagher, J. B. *Antarctic Nutrient Cycles and Food Webs* (eds. W. R. Siegfried, P. R. Condy, & R. M. Laws) (Springer, 1985).

75 Savvichev, A. S. *et al.* Microbial processes of the carbon and sulfur cycles in an ice-covered, iron-rich meromictic lake Svetloe (Arkhangelsk region, Russia). *Environ. Microbiol.* **19**, 659-672 (2007).
76 Tebo, B. M. Manganese (II) oxidation in the suboxic zone of the Black Sea. *Deep-Sea Res.* **38**, S883-S905 (1991).
77 Su, J. *et al.* CotA, a multicopper oxidase from *Bacillus pumilus* WH4, exhibits manganese-oxidase activity. *PLoS One* **8**, e60573 (2013).
78 Su, J. *et al.* Catalytic oxidation of manganese (II) by multicopper oxidase CueO and characterization of the biogenic Mn oxide. *Water Res.* **56**, 304-313 (2014).

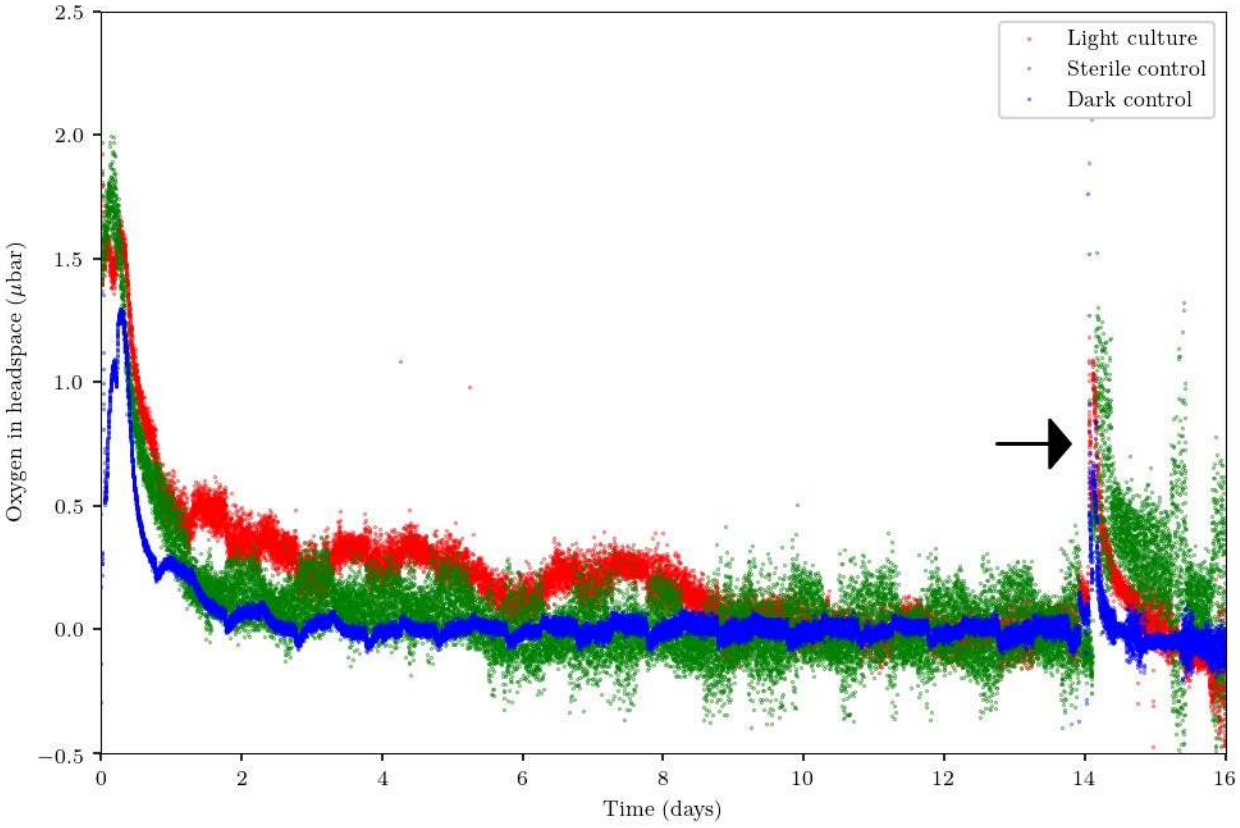

Extended Data Figure 1. Partial pressure of oxygen in the headspace of enrichment cultures and dark controls. Oxygen concentration (μatm) measured in the headspaces of 150 ml serum bottles that contained 100 ml of MFGL medium, 50 μM sulfide and 1 mM $MnCl_2$. One inoculated culture was incubated in the light (red points), another one) in the dark (blue points. The sterile control (green points) was incubated in the light. Individual points are measurements by the oxygen sensor taken each 48.2 s. To control for sensor drift and re-calibrate sensor zero point, the bottles were flushed with oxygen-free N_2 on day 14 (black arrow) after the inoculation. The fluorescence reading value after the stabilization was set as zero. The diurnal oscillations in O_2 concentration reflect temperature changes induced by the

proximity to the light bulb with a 12:12 h day/night cycle. Oxygen concentrations in all cultures were lower than 1 nmol at all times after ~ 12 h and before the flushing on day 14.

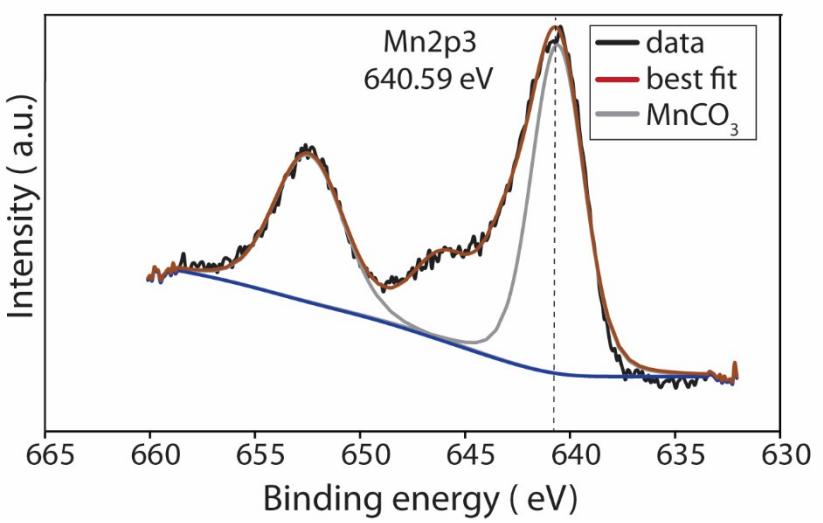

Extended Data Figure 2. X-ray photoelectron spectroscopy (XPS) analysis for the 2p spectral region of Mn in sterile control incubated in the light for two weeks. The $Mn2p_{3/2}$ main peak of the sample fits the $MnCO_3$ standard at binding energy of 640.59 eV that corresponds to the redox state of Mn(II).

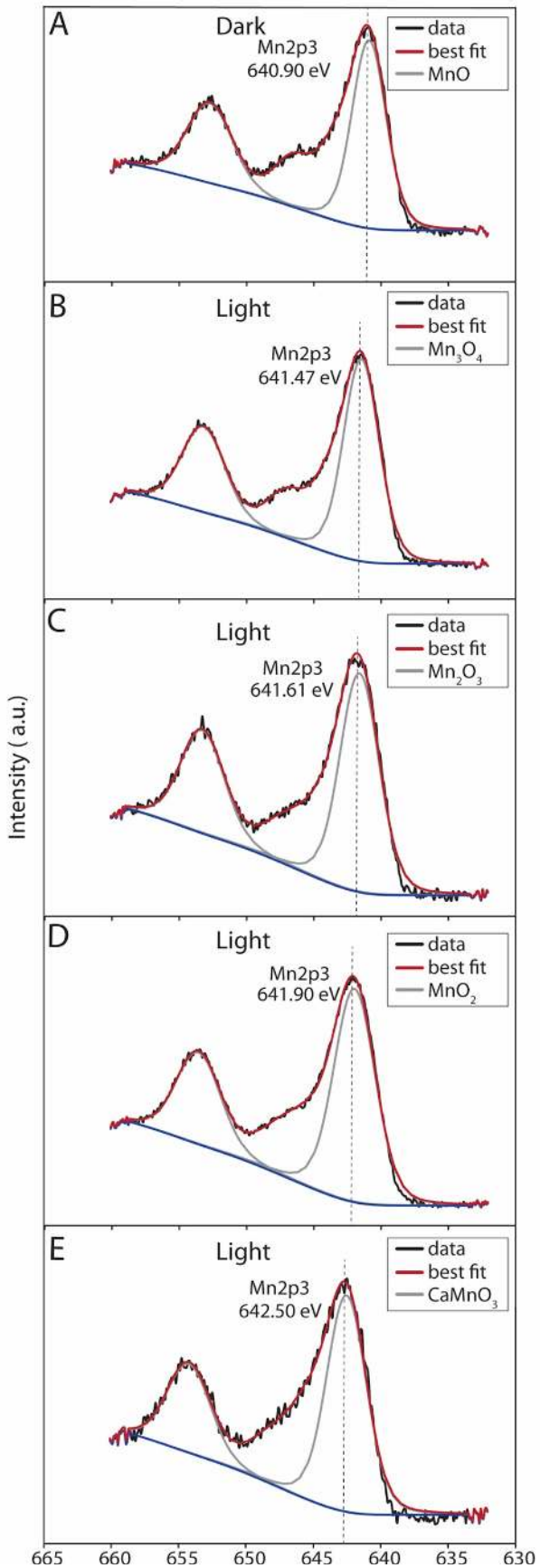
A
Dark
Mn2p3
640.90 eV
data
best fit
MnO
B
Light
Mn2p3
641.47 eV
data
best fit
Mn_3O_4
C
Light
Mn2p3
641.61 eV
data
best fit
Mn_2O_3
D
Light
Mn2p3
641.90 eV
data
best fit
MnO_2
E
Light
Mn2p3
642.50 eV
data
best fit
$CaMnO_3$
Intensity (a.u.)
665
660
655
650
645
640
635
630

Extended Data Figure 3. X-ray photoelectron spectra (XPS) of the 2p spectral region of Mn in two-week old microbial cultures. A: Biofilm incubated in the dark. The $Mn2p_{3/2}$ main peak of the sample fits the MnO standard at binding energy of 640.90 eV that corresponds to the redox state of Mn(II). B: Biofilm incubated in the light. The $Mn2p_{3/2}$ main peak of the sample fits the Mn_3O_4 standard at binding energy of 641.47 eV that corresponds to Mn(III) and Mn(II). C: Biofilm incubated in the light (a different region). The $Mn2p_{3/2}$ main peak of the sample fits the Mn_2O_3 standard at binding energy of 641.61 eV that corresponds to Mn(III). D: Biofilm incubated in the light (a different region). The $Mn2p_{3/2}$ main peak of the sample fits MnO_2 standard at binding energy of 641.90 eV that corresponds to redox state of Mn(IV). E: Biofilm incubated in the light. The $Mn2p_{3/2}$ main peak of the sample fits the $CaMnO_3$ standard at binding energy of 642.50 eV that corresponds to Mn(IV).

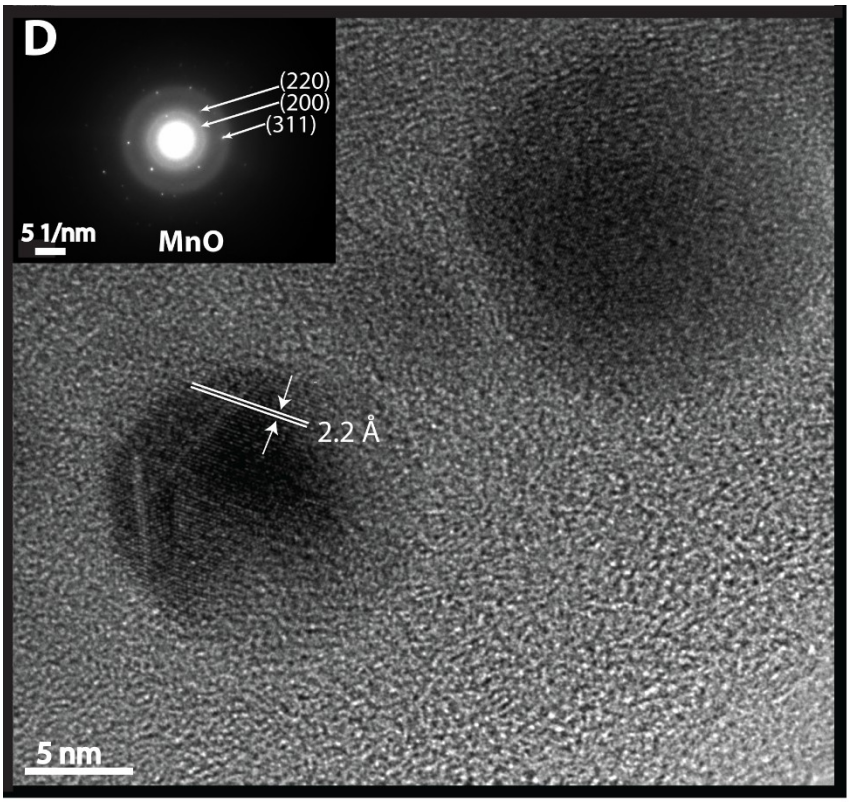

Extended Data Fig. 4. HRTEM and SAED of minerals found within biofilms, but not on cell surfaces. The indexes of the SAED pattern correspond to MnO with d-spacing of 2.2 Å.

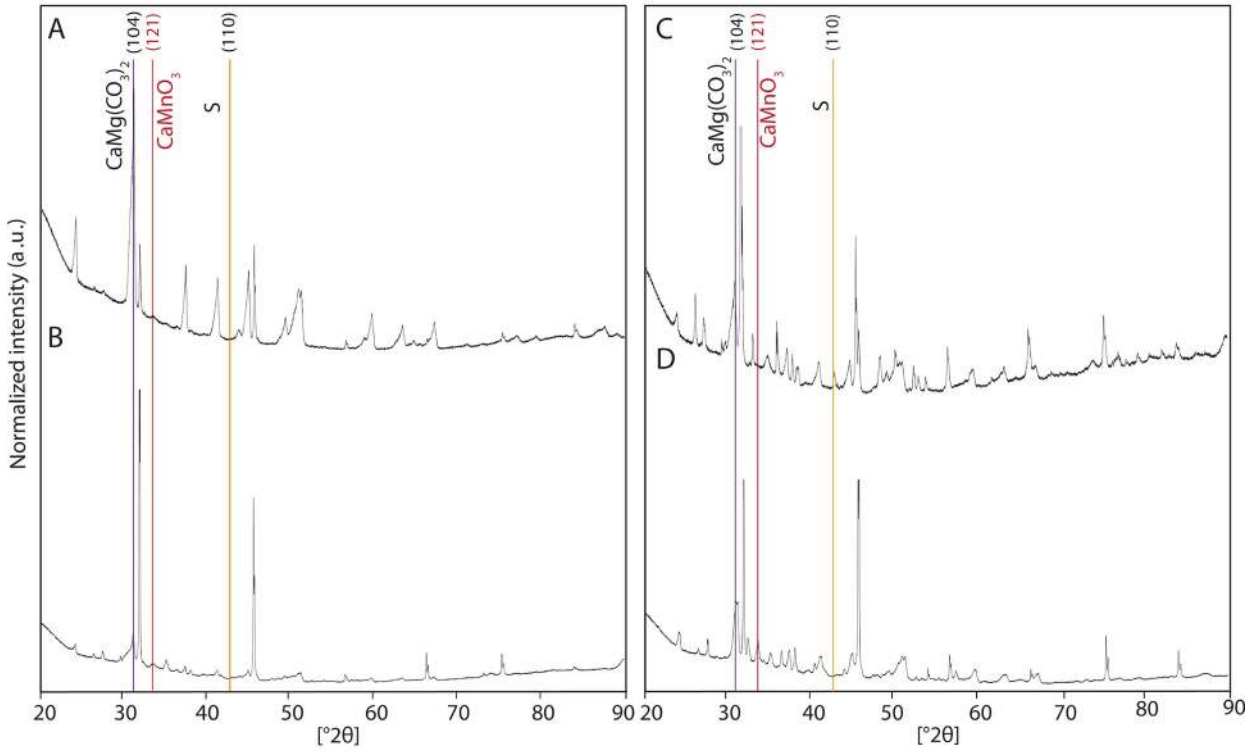

Extended Data Figure 5. X-ray diffraction spectra of biofilm samples incubated in the light for two weeks. These biofilms were not treated to remove manganese oxides before inoculation. A: 1 mM Mn(II) and 0.05 mM Na_2S. B: 0.1 mM Mn(II) and 0.05 mM Na_2S. C: 1 mM Mn(II) and 1 mM Na_2S. D: 1 mM Mn(II) and 0.25 mM Na_2S. Purple line shows the highest intensity peak at 2Θ of 30.870° for the basal reflection of (104) plane of dolomite, $CaMg(CO_3)_2$. Red line shows the highest intensity peak at 2Θ of 33.867° for the basal reflection of (121) plane of $CaMnO_3$. Orange line shows the highest intensity peak at 2Θ of 42.845° for the basal reflection of (110) plane of elemental sulfur, S°.

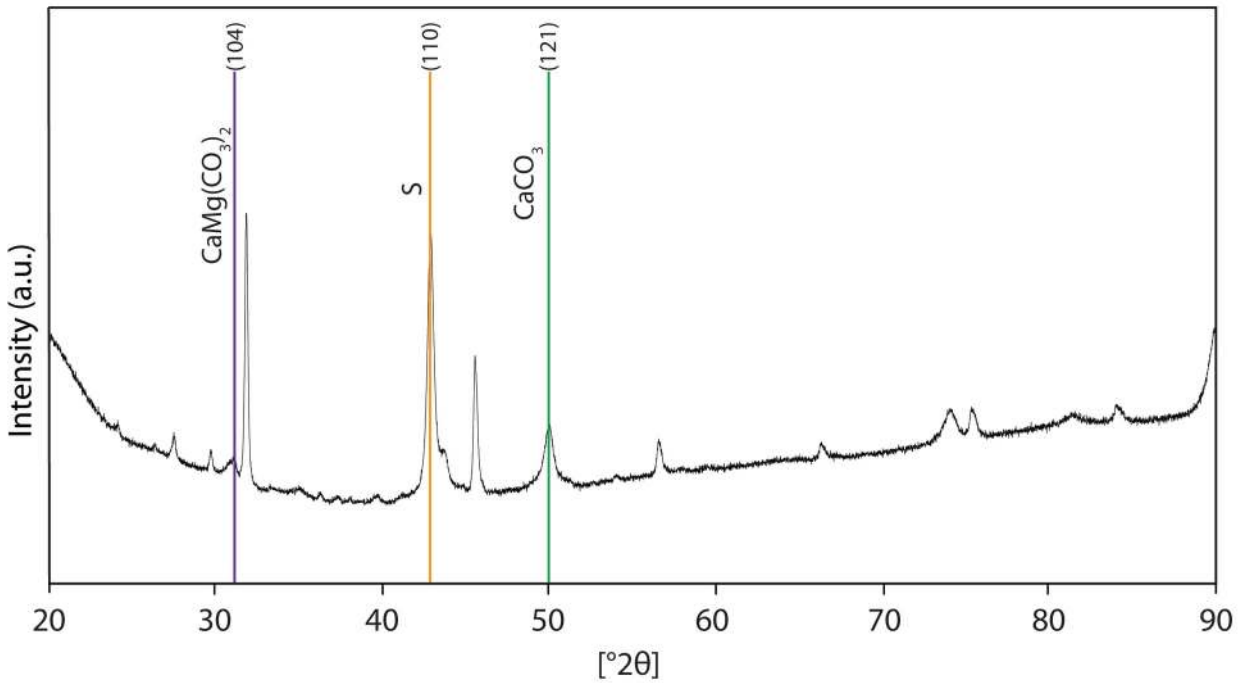

Extended Data Figure 6. XRD of a biofilm incubated with 0.05 mM Na_2S and no Mn(II) in the light for 2 weeks. The inoculum for this experiment was not treated to remove manganese oxides. Purple line shows the highest intensity peak at 2Θ of 30.870° for the (104) basal reflection of $CaMg(CO_3)_2$. Orange line shows the highest intensity peak at 2Θ of 42.845° for the (110) basal reflection of S°. Green line shows the highest intensity peak at 2Θ of 51.051° for the (121) basal reflection of $CaCO_3$.

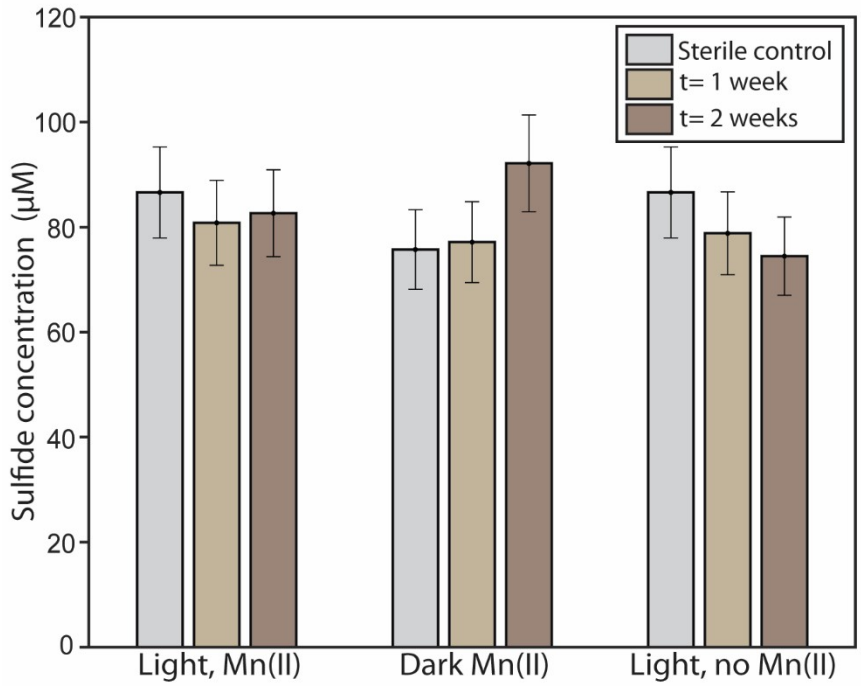

Extended Data Figure 7. Sulfide concentration in biofilms and sterile controls over the course of a two-week experiment. "Light, Mn" refers to biofilms grown with 1 mM Mn(II) and 0.05 mM initial Na_2S. "Dark, Mn" refers to biofilms grown with 1 mM Mn(II) and 0.05 mM initial Na_2S in the dark. "Light, no Mn" refers to biofilms grown in the light at a 12:12h day/night cycle without added $MnCl_2$ and with 0.05 initial mM Na_2S. The uninoculated media (sterile controls) were incubated under chemical and physical conditions that matched the corresponding cultures (dark, light, no added manganese beyond that in the trace metal solution). The concentrations of sulfide in sterile controls were measured after two weeks. Error bars show standard deviations in triplicate bottles.

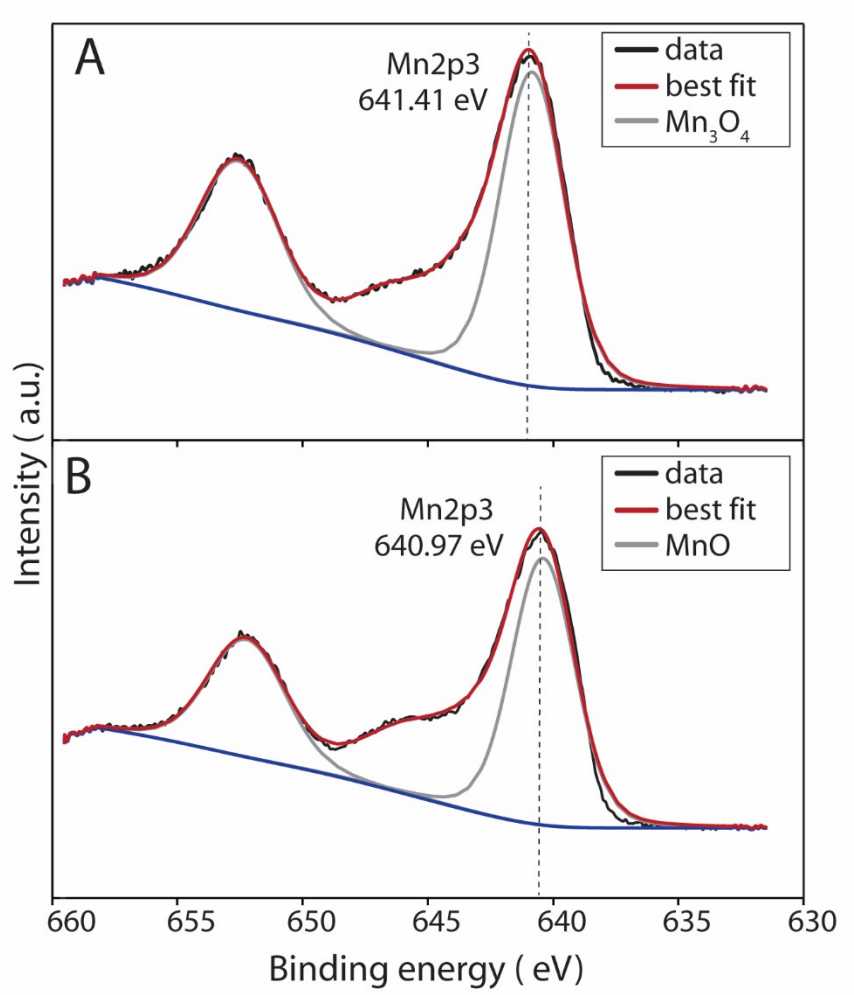

Extended Data Figure 8. Test of Mn-oxidizing activity in cell suspensions of photosynthetic cultures enriched under two different conditions. Shown are results of XPS analysis of the 2p spectral region of Mn. A. Culture enriched on 1 mM Mn(II) and 0.05 mM H_2S (Condition 1). The $Mn2p_{3/2}$ main peak of the sample fits Mn_3O_4 standard at binding energy of 641.41 eV. This corresponds to Mn(II) and Mn(III). B: Culture enriched on 1 mM H_2S (Condition 2). The $Mn2p_{3/2}$ main peak of the sample fits MnO standard at binding energy of 640.97 eV and corresponds to the redox state Mn(II). Detailed experimental protocol is described in section 2.2. and summarized in Extended Data Table 3.

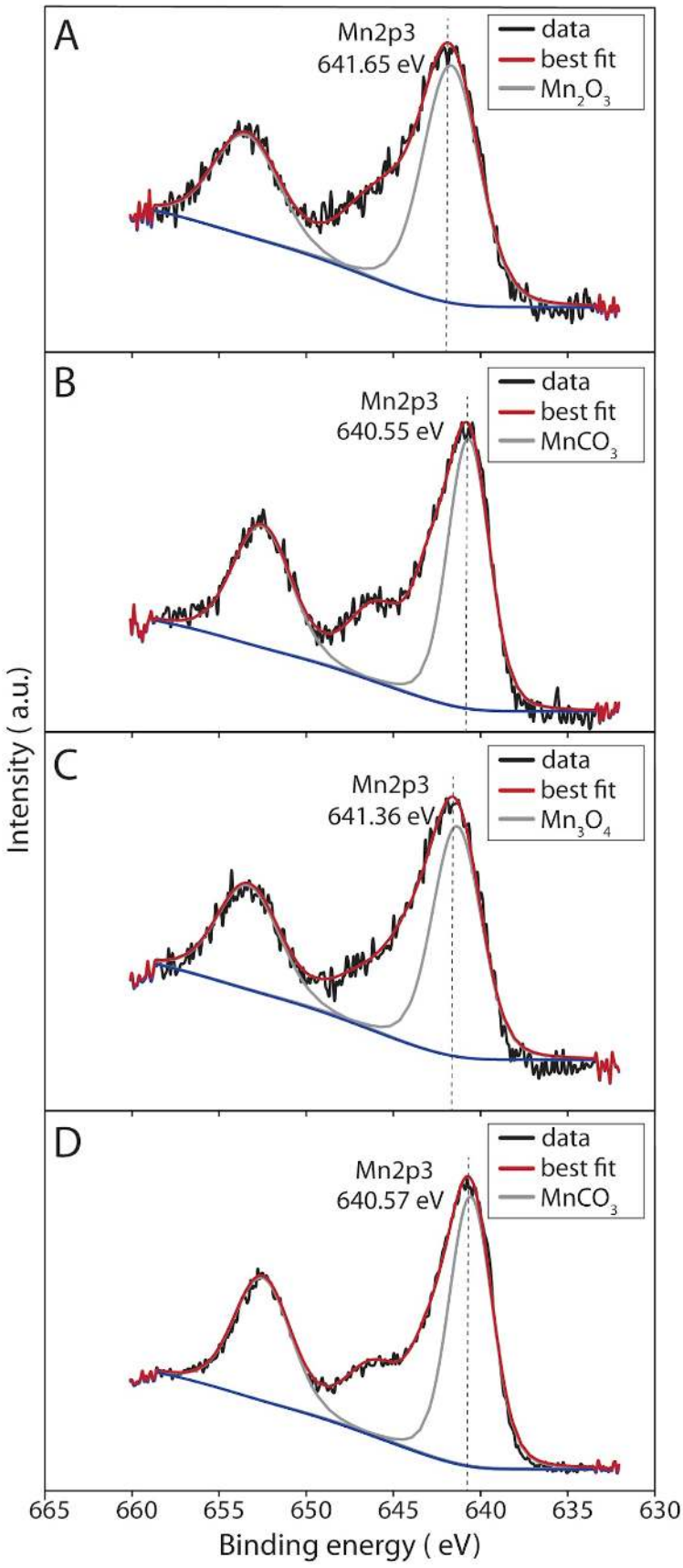
A
Mn2p3
641.65 eV
data
best fit
Mn2O3
B
Mn2p3
640.55 eV
data
best fit
MnCO3
C
Mn2p3
641.36 eV
data
best fit
Mn3O4
D
Mn2p3
640.57 eV
data
best fit
MnCO3
Intensity (a.u.)
665
660
655
650
645
640
635
630
Binding energy (eV)

1048

Extended Data Figure 9. Test of Mn-oxidizing activity in cell suspensions of pure cultures and co-cultures of *Chlorobium limicola (Cl), Chlorobaculum tepidum (Ct),* and *Geobacter lovleyi (Gl)*. Shown are results of XPS analysis of the 2p spectral region of Mn. A. *Cl, Ct and Gl.* The $Mn2p_{3/2}$ main peak of the sample fits Mn_2O_3 standard at binding energy of 641.65 eV. This corresponds to a valence state of Mn(III). B: *Cl and Ct*. The $Mn2p_{3/2}$ main peak of the sample fits $MnCO_3$ standard at binding energy of 640.55 eV and corresponds to the redox state Mn(II). C: *Cl and Gl.* The $Mn2p_{3/2}$ main peak of the sample fits Mn_3O_4 standard at binding energy of 641.36eV. D: *Ct* and *Gl.* The $Mn2p_{3/2}$ main peak of the sample fits $MnCO_3$ standard at binding energy of 640.57 eV Detailed experimental protocol is described in section 2.2.1. All co-cultures were grown with 1 mM Mn(II) and 0.05 mM H_2S for 2 weeks in the light.

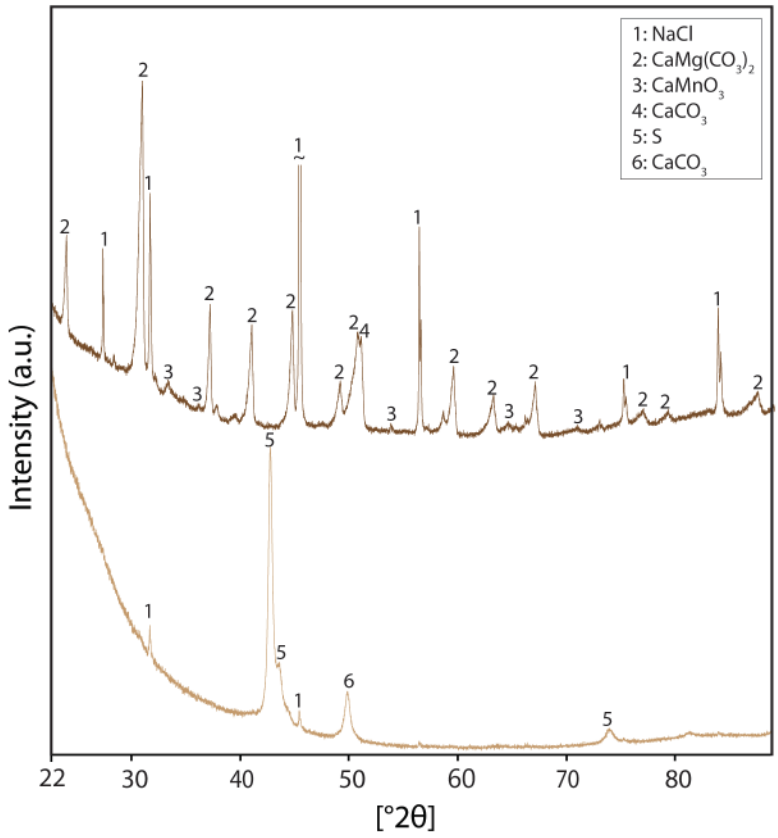

Extended Data Figure 10. X-ray diffraction spectra of biofilms. Top spectrum: biofilms incubated in the light for two weeks with 1 mM Mn(II) without the treatment to remove manganese oxides from the inoculum. The untreated biofilms contained dolomite ($CaMg(CO_3)_2$, "2"), manganese oxides ($CaMnO_3$, "3"), and aragonite ($CaCO_3$, "4"). Bottom spectrum: inoculum treated to remove the carry-over of manganese oxides before any incubation (see Methods section 1.1.1) contained sulfur; (S, "5") and calcium carbonate ($CaCO_3$, "6").

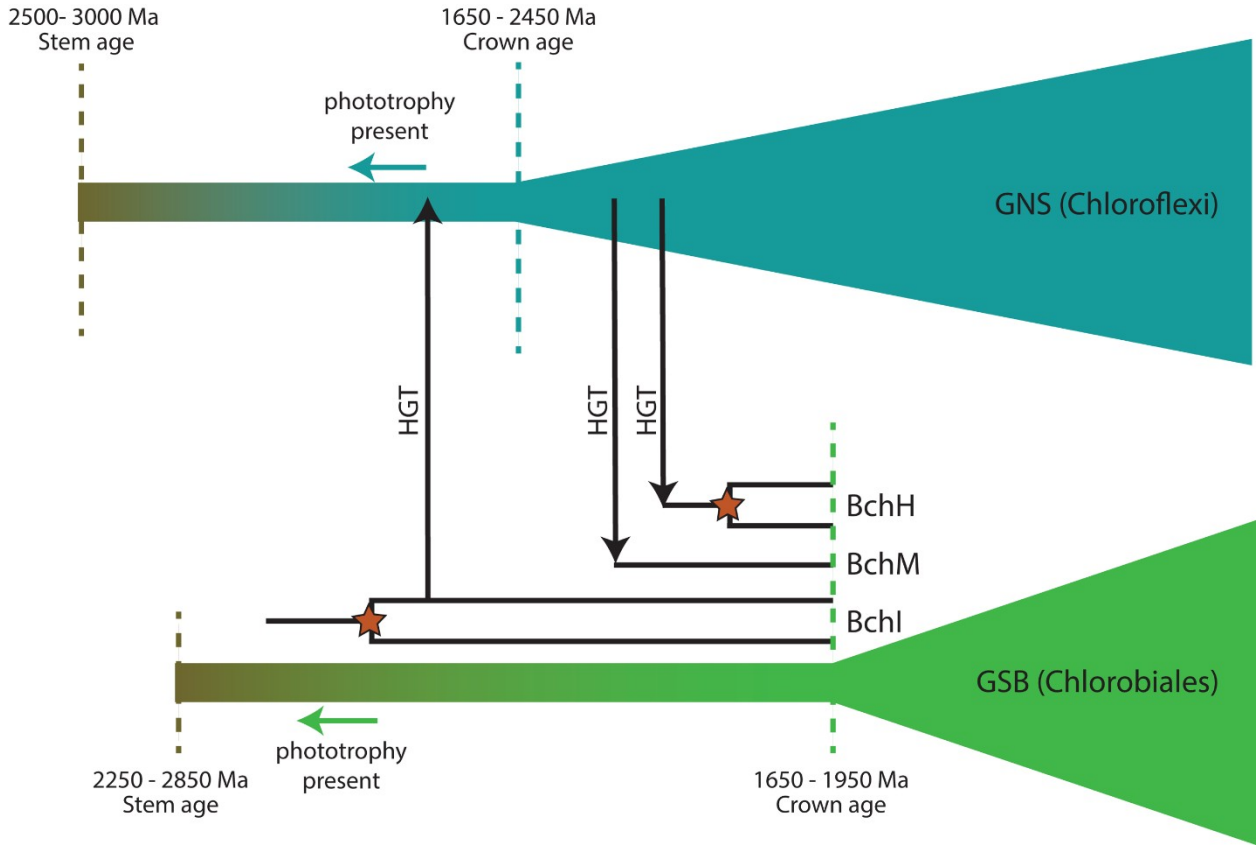

Extended Data Figure 11. Reticulate history of bacteriochlorophyll biosynthesis genes supports a long history of phototrophy in the Chlorobiales stem lineage. Horizontal gene transfers and gene duplications of bacteriochlorophyll genes were taken from[73], and age estimates for crown Chlorobi and GNS groups were taken from[28].

1076

1077

Extended Data Table 1. Aquatic environments with H_2S and Mn in the photic zone.

Water body	H_2S (µM)	Mn(II) (µM)	Photic Zone	Reference
Lake A	230	140	Green Sulfur Bacteria	[70]
Lake Vanda	240	120	Unclear	[71]
Garrow Lake	20	18	Green Sulfur Bacteria	[72]
Sombre Lake	1.2	68	Green Sulfur Bacteria	[73]
Svetloe Lake	2	60	Green Sulfur Bacteria	[74]
Black Sea	2	8.4	Green Sulfur Bacteria	[75]
Green Lake	20-30	50-60	Green Sulfur Bacteria	[9]

Extended Data Table 2. Shake tube and transfer procedures used to obtain enrichments from conditions 1 and 2.

First round shake tube	Incubation period, (days)	Colonies	Transfer into liquid medium	Incubation period (days)	Growth[1]	Enrichment
20 µM Na_2S, 1 mM $MnCl_2$	30	Black and dark brown	Brown colony; 0.02 mM Na_2S, 1 mM $MnCl_2$	30	+	Condition 1
1 mM Na_2S	30	Black, white and dark brown	Brown colony; 1 mM Na_2S	30	+++	Condition 2
Second round shake tube	**Incubation period (days)**	**Colonies**	**Transfer into liquid medium**	**Incubation period (days)**	**Growth[1]**	**Enrichment**
0.02 mM Na_2S, 1 mM $MnCl_2$	30	Brown, dark brown	Brown colony; 0.02 mM Na_2S, 1 mM $MnCl_2$	30	+	Condition 1
1 mM Na_2S	30	Brown, dark brown	Brown colony; 1 mM Na_2S	30	+++	Condition 2

[1]Growth of colonies transferred from shake to liquid media of same chemical composition; '+' signifies low micr
'+++' signifies high microbial growth. [2]Microbial composition determined by metagenomic sequencing. [3]*Achole*

75
76

equifetale, Alistipes sp. HGB5, and Caldicoprobacter oshimai.

Extended Data Table 3. Summary of the methods used to examine the redox state of manganese in enrichment cultures.

Enrichment condition	Transfer condition	Transfer MFGL medium composition	Incubation time (days)	Growth[1]	Mn oxidation activity[2]
Condition 1	Cell suspension	0.02 mM Na_2S, 1mM $MnCl_2$	3	-	+
Condition 2	Cell suspension	0.02 mM Na_2S, 1 mM $MnCl_2$	3	-	-
Condition 1	5 % inoculum	0.02 mM Na_2S, 1mM $MnCl_2$	7	-	-
Condition 2	5 % inoculum	0.02 mM Na_2S, 1mM $MnCl_2$	7	+	-

[1]The + or – indicates visible growth of the co-culture, [2]Manganese oxidation in the enrichment cultures was examined using XPS; + or – signifies the presence or absence of Mn(II) oxidizing activity in the microbial co-culture.

Extended Data Table 4. Mn(II) oxidation genes with confirmed function compared using BLASTp v. 2.6.0+ against *Chlorobium limicola* SR-12 genome.

Locus ID	Gene Annotation	Gene Name	Organism	Ref.	% identity
PputGB1_3353	animal heme peroxidase	*mopA*	*Pseudomonas putida*	[19]	46
WP_007817484	animal heme peroxidase	*ahpL*	*Roseobacter* sp. AzwK-3b	[20]	40
WP_009209951	animal heme peroxidase	*mopA*	*Aurantimonas manganoxydans*	[53]	47
WP_006837219	multi-copper oxidase	*mnxG*	*Bacillus* sp. strain SG-1	[18]	no hits
WP_076798083	multi-copper oxidase / billirubin oxidase	*boxA*	*Arthrobacter* sp. QXT-31	[34]	no hits
AFL56752	multi-copper oxidase, type 2	*cotA*	*Bacillus pumilus* WH4	[77]	no hits
CAJ19378	multi-copper oxidase	*moxA*	*Pedomicrobium* sp. ACM 3067	[52]	no hits
NP_745328	multi-copper oxidase / billirubin oxidase	*mcoA*	*Pseudomonas putida*	[19]	no hits
EG12318	multi-copper oxidase	*cueO*	*Escherichia coli*	[78]	no hits

Note: All AHPs also hit hemolysin-type calcium-binding region in *Chlorobium limicola* (E-value 3e-21, bit scor